U.S. DEPARTMENT OF ENERGY

PNNL-16727

Prepared for the U.S. Department of Energy
under Contract DE-AC05-76RL01830

Long-Term Modeling of Solar Energy: Analysis of Concentrating Solar Power (CSP) and PV Technologies

Y Zhang
SJ Smith

August 2008

Pacific Northwest
NATIONAL LABORATORY

DISCLAIMER

PACIFIC NORTHWEST NATIONAL LABORATORY
operated by
BATTELLE
for the
UNITED STATES DEPARTMENT OF ENERGY
under Contract DE-AC05-76RL01830

Printed in the United States of America

Available to DOE and DOE contractors from the
Office of Scientific and Technical Information,
P.O. Box 62, Oak Ridge, TN 37831-0062;
ph: (865) 576-8401
fax: (865) 576-5728
email: reports@adonis.osti.gov

Available to the public from the National Technical Information Service,
U.S. Department of Commerce, 5285 Port Royal Rd., Springfield, VA 22161
ph: (800) 553-6847
fax: (703) 605-6900
email: orders@ntis.fedworld.gov
online ordering: http://www.ntis.gov/ordering.htm

This document was printed on recycled paper.
(9/2003)

PNNL-16727

Long-Term Modeling of Solar Energy: Analysis of Concentrating Solar Power (CSP) and PV Technologies

Y Zhang
SJ Smith

August 2008

Prepared for the U.S. Department of Energy
under Contract DE-AC05-76RL01830

Pacific Northwest National Laboratory
Richland, Washington 99352

Long-Term Modeling of Solar Energy: Analysis of Concentrating Solar Power (CSP) and PV Technologies

Yabei Zhang
Steve Smith

Joint Global Change Research Institute, College Park, MD
January, 2008

Abstract

Solar technologies have unique characteristics that require detailed study to develop a suitable representation for modeling purposes. Solar technologies generally have low operating costs and carbon emissions, but high capital cost. Thus financing assumptions are particularly important for this type of capital-intensive technology. Intermittency is also a major characteristic of solar energy. In particular, when modeling solar energy, the interactions between solar generators and other generators in the electric system are critical in determining the long-term market potential for solar energy. This report includes three separate analyses developed to study these characteristics and guide the implementation of solar energy under JGCRI's ObjECTS MiniCAM framework: (1) a review of the sensitivity of solar energy cost to different financial assumptions, (2) the development of a new approach to modeling CSP market potential considering intermittency, and (3) an analysis of the impact of intermittency of solar energy on system reliability. The current implementation of solar energy in the ObjECTS Framework is discussed at the end of the report along with preliminary model analysis results.

Table of Contents

List Of Figures

Tables

1 Introduction

Renewable energy is increasing as a component of the energy supply portfolio, contributing to energy supply security and providing opportunities for mitigating greenhouse gases. As a part of the renewable family, solar energy, defined as solar radiation exploited for hot water production and electricity generation (IEA, 2007), has developed rapidly in recent years. In this chapter, we briefly review the current status of solar technologies. We also describe the general climate-change modeling framework that motivates this study. Finally, we provide brief previews of the report's chapters.

1.1 Development of Solar Energy

Solar is the world's most abundant, renewable source of energy. Every year, the sun irradiates the earth's land masses with the equivalent of 19 trillion tonnes of oil equivalent (toe). A small fraction of this energy could satisfy the world's energy requirements, around 9 billion toe per year (WEC, 2001). The challenge is harnessing solar energy in a cost-effective way.

Technology advances and policy supports are major drivers for the development of solar energy. According to the International Energy Agency (IEA) energy statistics, although solar energy only provides 0.039% of the world's total primary energy supply (TPES) (Figure 1-1), it had the second highest annual growth rate (28.1%) from 1971 to 2004 (Figure 1-2). Based on historical technology progress and cost reduction, some have predicted that over the next two decades solar energy will increasingly become a competitive choice for electricity and energy applications.

There are three major ways to use solar energy: photovoltaic (PV) systems that convert light directly into electricity, solar water heating systems that use sunlight to heat water, and solar thermal systems that concentrate solar radiation into a small space and produce high temperatures, which use this heat to operate a conventional power cycle. We focus our study here on grid-connected electricity generated using concentrating thermal solar power (CSP) and grid-connected photovoltaics (PVs).

What is the role of solar energy in the long term? According to the Office of Energy Efficiency and Renewable Energy (EERE) of the US Department of Energy (2006), to be competitive in the long term (10–15-year horizon), the cost of utility grid-connected PV

and CSP needs to be reduced to $0.10-0.15/kWh and $0.05-0.08/kWh[1], respectively. What will be the market share of these energy technologies if such goals are achieved? How will solar energy contribute to greenhouse gas reductions? These questions can be analyzed using the Mini Climate Assessment Model (MiniCAM) developed by the Joint Global Change Research Institute (JGCRI).

1.2 ObjECTS MiniCAM Model

The Object-oriented Energy, Climate, and Technology Systems (ObjECTS) framework uses a flexible, object-oriented modeling structure to implement an enhanced version of the partial-equilibrium model MiniCAM (Kim et al. 2006). The ObjECTS MiniCAM is an integrated model of the economy, energy supply and demand technologies, agriculture, land-use, carbon-cycle, and climate. This framework is intended to bridge the gap between "bottom-up" technology models and "top-down" macro-economic models. By allowing a greater level of detail where needed, while still enabling interaction between all model components, the ObjECTS framework allows a high degree of technological detail while retaining system-level feedbacks and interactions. By using object-oriented programming techniques (Kim et al. 2006), the model is structured to be data-driven, which means that new model configurations can be created by changing only input data without changing the underlying model code.

The MiniCAM is a partial-equilibrium model structure that is designed to examine long-term, large-scale changes in global and regional energy systems. The MiniCAM has a strong focus on energy supply technologies and has been recently expanded to include a comprehensive suite of end-use technologies. The MiniCAM was one of the models used to generate the IPCC SRES scenarios (Nakicenovic and Swart 2000). This model has been used in a number of national and international assessment and modeling activities such as the Energy Modeling Forum (EMF; Edmonds, et al. 2004, Smith and Wigley 2006), the U.S. Climate Change Technology Program (CCTP; Clarke et al. 2006), and the U.S. Climate Change Science Program (CCSP; Clarke et al. 2007) and IPCC assessment reports.

The MiniCAM model is calibrated to 1990 and 2005 and operates in 15-year time steps to the year 2095. It takes inputs such as labor productivity growth, population, fossil and non-fossil fuel resources, energy technology characteristics, and productivity growth rates and generates outputs of energy supplies and demands by fuel (such as oil and gas) and energy carriers (such as electricity), agricultural supplies and demands, emissions of

[1] The reason that PVs can compete at higher costs than CSPs is that PVs are less resource constrained and can usually be closer to transmission grids.

greenhouse gases (carbon dioxide, CO_2; methane, CH_4; nitrous oxide,N_2O), and emissions of other radiatively important compounds (sulfur dioxide, SO_2; nitrogen oxides, NO_X; carbon monoxide, CO; volatile organic compounds, VOC; organic carbon aerosols, OC; black carbon arosols, BC). The model has its roots in Edmonds and Reilly (1985), and has been continuously updated (Edmonds et al. 1996; Kim et al. 2006). MiniCAM also incorporates MAGICC, a model of the carbon cycle, atmospheric processes, and global climate change (Raper et al. 1996; Wigley and Raper 1992).

1.3 Chapter Highlights

This report includes three separate analyses developed to guide implementation of solar energy under the ObjECTS framework. However, because these analyses focus on methodological development, they may have applications in other settings. Solar technologies have some unique economic characteristics that need detailed study to develop representation and parameters for modeling. The three separate analyses focus on these unique characteristics.

In Chapter 2, we discuss how the levelized energy cost (LEC) is calculated and how different methodologies and assumptions can change the LEC substantially. LEC is a widely used indicator to compare the competitiveness of different energy sources. One feature of solar energy is its low operating cost, with a relatively high capital cost. Thus financing assumptions are particularly important for this type of capital-intensive technology. Using a 100-MW CSP plant as an example, we calculate LEC from both the private perspective and the public perspective. We find that the results from the two methodologies are fairly comparable under certain assumptions. However, the LEC from the private perspective is very sensitive to financing assumptions and policy incentives towards CSPs (e.g. tax credits and favorable depreciation schedules). Thus, special attention should be given to these assumptions when comparing LECs from different sources.

Intermittency is a major characteristic of solar energy and also a major challenge when modeling solar energy. Because we model grid-connected solar electricity, the interactions between solar generators and other generators in the electric system become particularly important. Chapters 3 and 4 deal with intermittency for CSP and PV systems, respectively.

In Chapter 3, we develop a methodology to calculate CSP electricity costs considering intermittency. We find a strong dependency of the CSP electricity cost on CSP market penetration when the CSP market penetration is high. This is partly due to the increasing

need for the backup output when the irradiance is low or unavailable, and partly due the loss of CSP output from the solar component when there is excess supply. Because the CSP backup component is powered by fossil fuel, this means that the effectiveness of using CSP to reduce carbon emissions decreases as the CSP market penetration level passes a certain threshold. Using the examples of San Diego and Phoenix, we find that this threshold can be quite high, more than 40% of the total intermediate and peak electricity supply. Therefore, CSP has the potential to supply a significant share of electric demands without a significant penalty due to intermittency.

In Chapter 4, we analyze the impact of intermittency of solar energy on system reliability planning. We consider the impact of no/low sun days on system reserve margins. Using a stylized analysis, we find that when the market penetration of PV is low, the number of no/low sun days plays an important role in determining additional system reserve margin and therefore it should be a consideration in addition to average irradiance level when selecting locations for PV systems. When the market penetration of PV is high, the requirement for additional system reserve margin can converge to one-to-one backup, which will significantly increase PV electricity cost.

Chapter 5 describes the current implementation of solar energy in the ObjECTS Framework. The results presented in the previous sections have been used to guide both a general implementation of solar energy and a specific incorporation of CSP solar technology.

Acknowledgements

The authors would like to thank Marshall Wise, Katherine Calvin, and April Volke for comments on draft versions of the report and G. Page Kyle for invaluable assistance in the construction of ObjECTS model input files. This work was funded by the U.S. Department of Energy's Office of Energy Efficiency and Renewable Energy with additional support from the California Energy Commission and the Global Energy Technology Strategy Program (GTSP).

Figure 1-1. 2004 Fuel Shares of World Total Primary Energy Supply (TPES)*

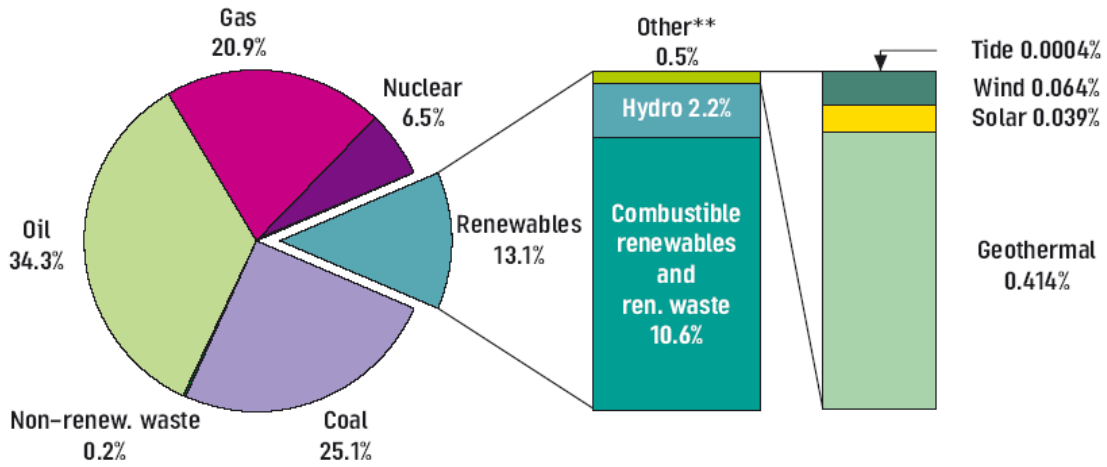

* TPES is calculated using the IEA conventions (physical energy content methodology). It includes international marine bunkers and excludes electricity/heat trade. The figures include both commercial and non-commercial energy.
** Geothermal, solar, wind, tide/wave/ocean.
Totals in graph might not add up due to rounding.
Source: IEA Energy Statistics

Figure 1-2. Annual Growth of Renewables Supply from 1971 to 2004

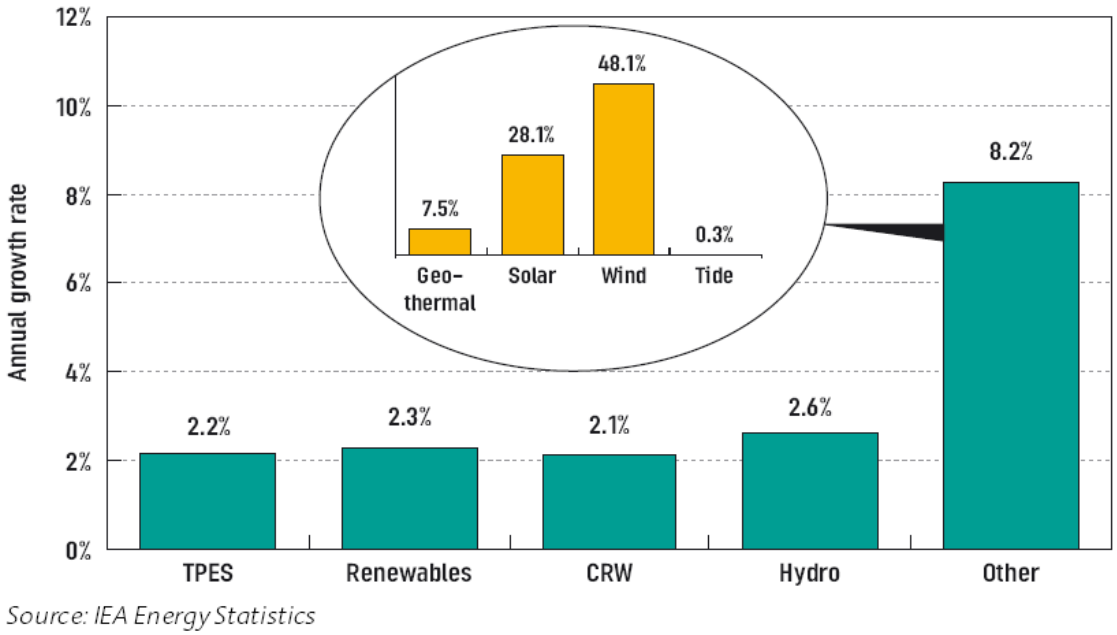

Source: IEA Energy Statistics

References

Bradford, Travis (2006). *Solar Revolution: The Economic Transformation of the Global Energy Industry*. MIT Press.

Clarke, L. E., M. A. Wise, J. P. Lurz, M. Placet, S. J. Smith, R. C. Izaurralde, A. M. Thomson, and S. H. Kim. 2006. "Technology and Climate Change Mitigation: A Scenario Analysis." PNNL-16078.

Clarke, L., J. Edmonds, J. Jacoby, H. Pitcher, J. Reilly, R. Richels. 2007. *Scenarios of Greenhouse Gas Emissions and Atmospheric Concentrations.* Report by the U.S. Climate Change Science Program and approved by the Climate Change Science Program Product Development Advisory Committee (United States Global Change Research Program, Washington, D.C.).

Edmonds J. A., J. F. Clarke, J. J. Dooley, S. H. Kim, and S. J. Smith. 2004. "Modeling Greenhouse Gas Energy Technology Responses to Climate Change." *Energy* 29 (9-10): 1529–1536.

Edmonds, J., and J. Reilly. 1985. *Global Energy: Assessing the Future.* Oxford, United Kingdom: Oxford University Press.

Edmonds, J. A., M. Wise, H. Pitcher, R. Richels, T. Wigley, and C. MacCracken. 1996. "An integrated assessment of climate change and the accelerated introduction of advanced energy technologies: An application of MiniCAM 1.0." *Mitigation and Adaptation Strategies for Global Change* 1 (4): 311–339.

EERE (2006). *Solar Energy Technologies Program, Multi-Year Program Plan 2007-2011*. Energy Efficiency and Renewable Energy, Department of Energy.

IEA (2007). *Renewables in Global Energy Supply- An IEA Fact Sheet* http://www.iea.org/textbase/papers/2006/renewable_factsheet.pdf

Kim, Edmonds, Lurz, Smith, and Wise (2006). "Hybrid Modeling of Energy-Environment Policies: Reconciling Bottom-up and Top-down." *The Energy Journal*, 2006.

Nakicenovic, N., and R. Swart, eds. 2000. *Special Report on Emissions Scenarios*. Cambridge, U.K.: Cambridge University Press.

Raper, S. C. B., T. M. L. Wigley, and R. A. Warrick. 1996. "Global sea level rise: Past and future." In *Sea-Level Rise and Coastal Subsidence: Causes, Consequences and Strategies.* (Milliman, J. D., and B. U. Haq, eds.). Kluwer Academic Publishers. 11–45.

Smith, S. J., and T. M. L. Wigley. 2006. "Multi-Gas Forcing Stabilization with the MiniCAM." *The Energy Journal* Special Issue #3.

Wigley, T. M. L., and S. C. B. Raper. 1992. "Implications for Climate and Sea-Level of Revised IPCC Emissions Scenarios." *Nature* 357 (6376): 293–300.

World Energy Council (2001). *Survey of Energy Resources 2001*.

2 Levelized Energy Cost: Sensitivity Study

2.1 Introduction

Levelized energy cost (LEC) is often used to compare competing energy sources. It is especially important for renewable energy due to its capital intensive nature. Experience has illustrated that the calculation of LEC for renewable energy sources is both complex and often subject to debate. Moreover, results can be significantly influenced by the methodology and the assumptions employed. For example, the first version of Sargent and Lundy's report, *Assessment of Concentrating Solar Power Cost and Performance Forecasts* (2002), was criticized for the use of some unrealistic financing assumptions and the absence of a sensitivity study on financial parameters (BEES, 2002). This chapter documents a methodology for calculating LEC using a standard 100-MW concentration solar power (CSP) plant as an example and focuses on sensitivity analysis.

2.2 LEC Definition

A levelized unit cost is a delivered product unit cost that, if charged for each year's production over the analysis period, would yield the same net present value of revenues as if the actual annual cost for each alternative were collected instead over the period. It is C in the following equation:

(2-1)

$$\sum_{i=1}^{n} \frac{CE_i}{(1+r)^i} = \sum_{i=1}^{n} \frac{C_i E_i}{(1+r)^i}$$

where C is a constant \$/kWh cost to be charged each i^{th} year over the analysis period (n=30 years, for example), E_i is the kWh generated in each such year, and C_i is the actual annual \$/kWh for each year, comprised of a current expense for fuel, labor, etc. plus a component for recovery of the investment cost, which may be a level series or may vary through time in some fashion.

Equation (2-1) can also be written as

(2-2)

$$C = \frac{\sum_{i=1}^{n} \frac{C_i E_i}{(1+r)^i}}{\sum_{i=1}^{n} \frac{E_i}{(1+r)^i}}$$

Since the term C_iE_i is dollars for each year, and the $1/(1+r)^i$ is a discount factor, the top of the right side can be interpreted as the present value of revenue requirements. The bottom is denominated in kWh and can be interpreted as the present value of energy. This is why LEC is often stated as the present value of costs divided by the present value of energy.

2.3 Public vs. Private Perspective

The choice of analytical perspective is critical because there is an important distinction in the calculations from a public perspective as compared to a private perspective. The basis for conducting private sector analysis includes market prices, taxes, depreciation, private cost of capital, and applicable incentives. The financial analysis for the private sector attempts to determine the actual costs and revenues that will be realized by the investor. Because solar projects are very capital intensive, the LEC from the private perspective is particularly sensitive to financing conditions and tax policies.

The economic analysis for the public sector is from the perspective of society as a whole. It ignores the effect of taxes and uses a social discount rate instead of a discount rate reflecting the cost of borrowing and desired returns (the latter is usually larger). In the following example, we compute the LEC from both the public and private perspectives for comparison.

2.4 CSP LEC Calculation Using Private Financial Analysis

For this analysis, we adopted the Independent Power Producer (IPP) Project Finance Model initially developed by Ryan Wiser of LBL and revised by Henry Price of NREL. The technology we consider is a trough hybrid solar plant with capacity of 100 MW. However, the general conclusion is not technology specific. The detailed baseline assumptions and results are presented in

Table 2-1.

The bolded figures are key assumptions for LEC calculation using private financial analysis. Except for solar irradiance level, they are primarily financing assumptions including financing structure, tax incentives, and the depreciation method.

In terms of financing structure, the baseline assumes IPP project finance. There are two major financing structures: corporate finance and project finance. Corporate financing, also known as internal or equity financing, is characterized by the use of corporate credit and general assets of a corporation, typically a utility, as the basis for credit and collateral. Because the overall credit rating of the company is used to estimate debt and equity costs rather than project specific capital costs, the cost of financing is low due to a better credit standing. However, because of high investment costs, most of the utilities are not able to generate sufficient corporate finance resources for solar projects (Kistner and Price, 1999). Thus, project finance is often used in long-term capital-intensive infrastructure and industrial projects such as solar power projects.

Project finance can be defined as the arrangement of debt, equity, and credit enhancement for the construction of a particular facility in a capital-intensive industry where lenders base credit appraisals on the estimated cash flows from the facility rather than on the assets or credit of the promoter of the facility (Short et al, 1995). It is more complicated and more expensive compared to corporate finance. Project finance is the primary financing structure used by IPPs.

The cost of raising capital, which can be measured as the internal rate of return (IRR) for equity investors and interest rate for lenders, depends on real and perceived technology risk, type of finance, and debt-equity ratio. Our baseline assumes 60% debt and 40% equity, which has a reasonable debt/equity ratio for IPP projects. Because a nominal IRR between 16%-20% is generally expected from IPP projects (Kistner and Price, 1999), our baseline assumes a real IRR of 14%. Note that all our assumptions are in constant dollars without accounting for inflation. If we consider 2-3% inflation rate, this IRR falls in the above range. In addition, we assume 20-year debt with a 6% real interest rate, which is also reasonable for IPP projects in the US.

As part of risk management, lenders usually require a certain debt service coverage ratio (DSCR). The DSCR is the amount of cash/operating income available divided by debt payments. Lenders want to assure that during the entire project lifetime the cash generated always covers debt service. One of the most important loan requirements is the minimum annual debt service coverage ratio (MADSCR). Lenders normally require that during every stage of the project the annual DSCR never falls short of the MADSCR.

Many lenders require a MADSCR between 1.2 and 1.5, depending on specific project risks and contractual arrangements (Kistner and Price, 1999). Our baseline assumes that the MADSCR is 1.3.

In terms of tax incentives, the baseline assumes no tax incentives because the ObjECTS model is for long-term projections so we expect the government tax incentives would be phased out over time as a technology becomes widely used. However, we note that investment tax credit (ITC) currently serves as a major incentive for CSP investment. For example, the Energy Policy Act of 2005 offers 30% federal tax credits for solar projects beginning in January 2006 till 2007 and it was later extended until the end of 2008[2]. In addition, some states provide additional tax incentives for solar energy investment. For example, California offers 15% ITC for solar projects.

In terms of the depreciation method, the baseline assumes 5-year modified accelerated cost recovery system (MACRS), which means that the applicable capital cost is depreciated according to the 5-year MACRS schedule. The MACRS establishes a set of schedules for various types of property, ranging from 3 to 50 years, over which the property may be depreciated. We use the assumption of a 5-year MACRS because the current policy allows 5-year MACRS for solar, wind, and geothermal property placed in service after 1986[3] and most references also use this assumption. For comparison, the MACRS schedule for fossil fuel power plants is normally 15 or 20 years.

Solar irradiance level determines the total electricity output from the CSP, which in turn determines revenues from energy and the CSP LEC. The baseline assumes 7.65 kWh/m^2/day which represents the San Diego region. We use this assumption because this region is one of the most ideal areas for solar energy in the US and a number of studies on solar energy have focused on this region.

Using the baseline assumptions as shown in

[2] Source: http://www.seia.org/solarnews.php?id=128
[3] Source: http://www.dsireusa.org/library/includes/incentive2.cfm?Incentive_Code=US06F&State=Federal&currentpageid=1

Table 2-1, the calculated real CSP LEC is 2004$ 0.1608/kWh. To ensure the project is financially feasible, the first year electricity price needs to be 2004$ 0.1517/kWh. In addition, the MADCSR is 1.53, which meets the requirement of a 1.3 MADSCR.

The key assumptions discussed above can make a significant impact on the CSP LEC. Thus, we will conduct a sensitivity analysis in the following section to evaluate how LEC is affected by changing these assumptions.

Table 2-1. Estimation of LEC: Baseline Assumptions and Results

Variables	Value	Notes
Baseline Assumptions		
Reference Year Dollars	2004	Assumed
Capacity (MW)	100	Assumed
Direct Normal Irradiance (kWh/m^2/day)	**7.65**	Assumed
Annual Solar-to-Electric Efficiency	12.60%	Assumed
Capacity Factor w/o hybrid	0.28	Calculated
Increased Capacity Factor due to the backup fuel	0.02	Assumed
Capacity Factor w/ hybrid	0.30	Calculated
Capital Cost w/ hybrid ($/kW)	3486	Assumed
Solar Field Size (km^2)	0.69	Assumed
Land Area (km^2)	2.30	Assumed
Land cost ($/m^2)	0.49	Assumed
Land Cost (M$s)	1.14	Calculated
Allowance for Funds Used During Construction (AFUDC)	3.5%	Assumed
Const. Period/First Year of Op.	1	Assumed
Fixed O&M Expense ($/kW-yr)	47.87	Assumed
Variable O&M Expense ($/MWh)	2.72	Assumed
Share of Electricity Produced by Gas	7%	Calculated
Gas Conversion Efficiency	0.46	Assumed
Annual Fuel Usage (MMBtu)	131418	Calculated
Insurance (% of installed cost)	0.5%	Assumed
Effective Income Tax Rate	40.0%	Assumed
Investment Tax Credit/dep adj	**0.0%**	Assumed
Percentage of Capital Depreciation at 5-yr MACRS	**100%**	Assumed
Percentage of Capital Depreciation at 15-yr MACRS	0.0%	Assumed
Percentage of Capital Depreciation at 20-yr MACRS	0.0%	Assumed
Energy Price Escalation Rate	1.3%	Assumed
Equity Fraction	40%	Assumed
Debt Fraction	**60%**	Assumed
Interest Rate	**6%**	Assumed
Minimum Annual Debt Service Coverage Ratio (MADSCR)	1.3	Assumed
Equity Internal Rate of Return (IRR)	**14%**	Assumed

Discount Rate	9%	Assumed
Baseline Results		
Average Annual DSCR	1.79	Calculated
MADSCR	1.53	Calculated
First Year Electricity Price (2004 $/kWh)	0.1517	Calculated
Real LEC (2004 $/kWh)	0.1608	Calculated

2.5 Sensitivity Analysis

(1) Financing Structure

Table 2-2 and Figure 2-1 show the results of sensitivity analysis of the different financing structures. In addition to IPP financing, as we discussed earlier, the CSP plant may be owned and financed by utilities. If we use a typical financing structure for an investor-owned utility (IOU) with 50% debt, 30-year term, 4% interest rate, and 12% IRR, the LEC will decrease slightly to $0.1567/kWh. Furthermore, rather than using commercial financing, if we use municipal financing with 100% debt, 30-year term, and 3.5% interest rate, the LEC can decrease to only 52% of the baseline cost. However, it should be noted that the MADSCR is only 0.6 in this case, which means that operating income for certain periods is not high enough to pay for amortized annual debt. Therefore, the municipal financing structure has to have some special payment schedule or other arrangements to make it feasible. If we allow the debt ratio to change while keep other assumptions the same and assure a 1.3 MADSCR is met, the lowest real LEC would be $0.1508/kWh, 94% of the baseline.

In Figure 2-1 and subsequent figures, the shaded bar represents the case that the requirement of a 1.3 MADSCR is not met.

Costs of raising capital also depend on the debt-equity ratio. If we assume LEC is constant at the baseline level and the debt term and interest rate do not change, we can investigate how the IRR and the MADSCR change with respect to the equity share. The results of this sensitivity analysis are depicted in Figure 2-2. It shows that the IRR is negatively correlated to the equity share while the MADSCR is positively correlated to the equity share. The MADSCR often binds in the initial years of operation and restricts the amount of low-cost debt that can be used by the project. If lenders require restrictive MADSCR, front-loading of contract payments and/or a back loading of debt payment could help to achieve a higher level of debt leverage (Kistner and Price, 1999).

The interest rate reflects lender's perception of the project risk and market conditions. It is also a major determinant of the real LEC. Assuming debt-equity ratio and IRR do not vary, Table 2-3 and

Figure 2-3 show LEC's sensitivity to different interest rates. If we use a more conservative interest rate 4%, the LEC decreases to 95% of the baseline. If we use a higher interest of 10%, the LEC increases to 114% of the baseline. Compared to other assumptions, the LEC is only moderately sensitive to interest rates.

Table 2-2. LEC's Sensitivity to Type of Financing

Sensitivity to Type of Financing	**IPP** Debt: 60%, 20 yrs, i=6% Equity: 40%, IRR=14%	**IOU** Debt: 50%, 30 yrs, i=4% Equity: 50%, IRR=12%	**Muni** Debt: 100%, 30yrs, i=3.5%	**Optimal Debt Ratio** Debt: 65.2%, 20 yrs, i=6% Equity: 34.8%, IRR=14%
Real LEC (2004 $/kWh)	0.1608	0.1567	0.0843	0.1508
Relative Cost Comparing to the Baseline	100%	97%	52%	94%
MADSCR	1.53	2.36	0.6	1.3

Figure 2-1. LEC's Sensitivity to Type of Financing

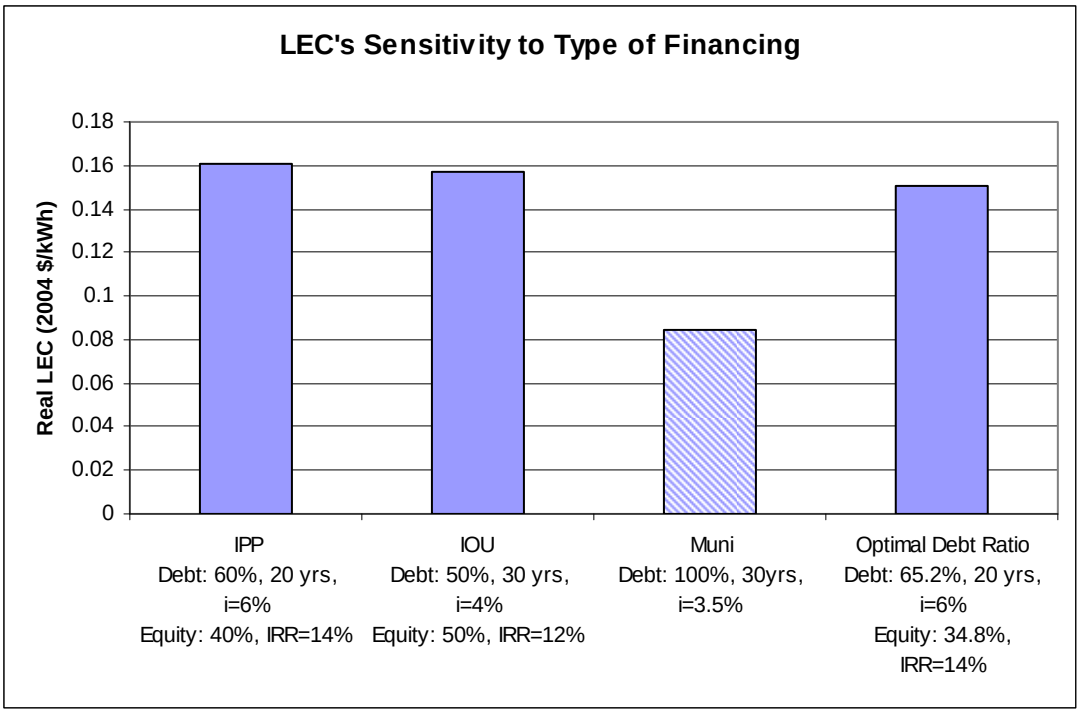

Figure 2-2. Equity Share Sensitivity Analysis

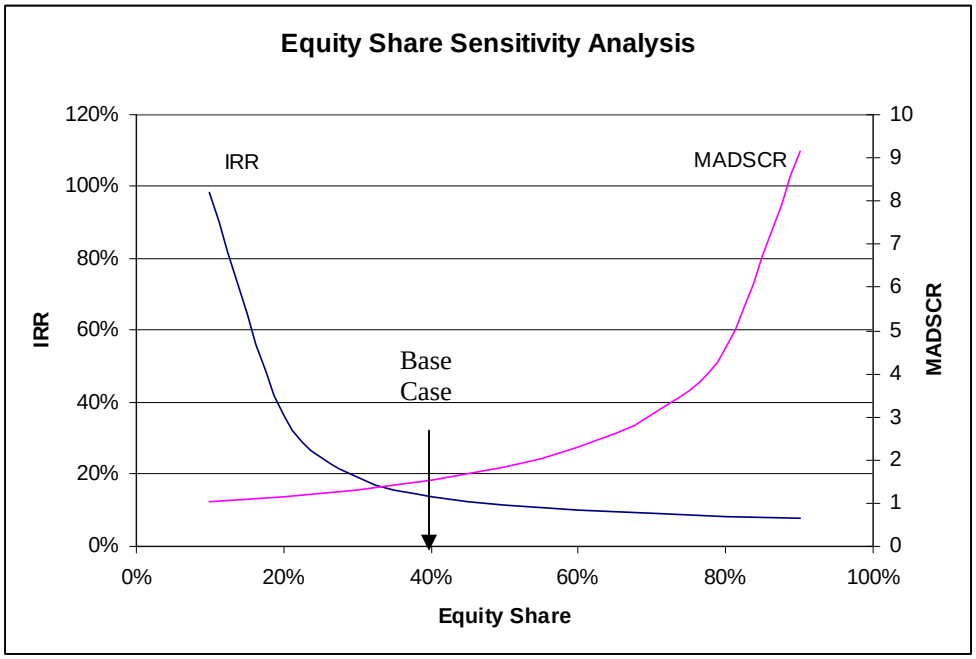

Table 2-3. LEC's Sensitivity to Interest Rate

Sensitivity to Interest Rate	6%	4%	8%	10%

Real LEC (2004 $/kWh)	0.1608	0.1535	0.1714	0.1828
Relative Cost Comparing to the Baseline	100%	95%	107%	114%
MADSCR	1.53	1.68	1.42	1.33

Figure 2-3. LEC's Sensitivity to Interest Rate

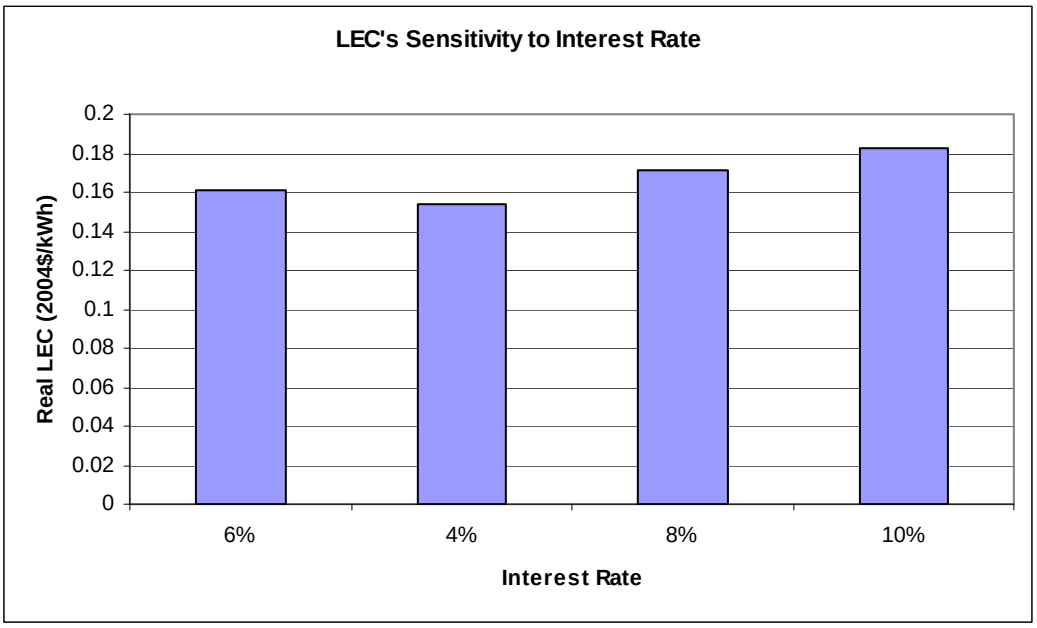

(2) Tax Incentives

Table 2-4 and Figure 2-3 show LEC's sensitivity to ITC incentives. If we assume 10% ITC, the LEC can decrease to $ 0.131/kWh. It can further decrease to $ 0.0714/kWh with

the assumption of 30% ITC which is only 44% of the baseline cost. However, we need to note that the MADSCR is 1.18 for the assumption of 10% ITC and only 0.46 for the assumption of 30% ITC. Without changing the financing structure or having other special payment arrangements, these LECs are difficult to realize in practice. If we require a MADSCR of 1.3 and allow the financing structure to change (equity share increases to 58.8%) we can get a LEC of $0.1077/kWh in the case of 30% ITC.

Table 2-4. LEC's Sensitivity to ITC Incentives

Sensitivity to ITC Incentives	0% ITC	10% ITC	30% ITC	30% ITC*
Real LEC (2004 $/kWh)	0.1608	0.131	0.0714	0.1077
Relative Cost Comparing to the Baseline	100%	81%	44%	67%
MADSCR	1.53	1.18	0.46	1.3

* equity share increased to 58.8%, other assumptions remain.

Figure 2-4. LEC's Sensitivity to ITC Incentives

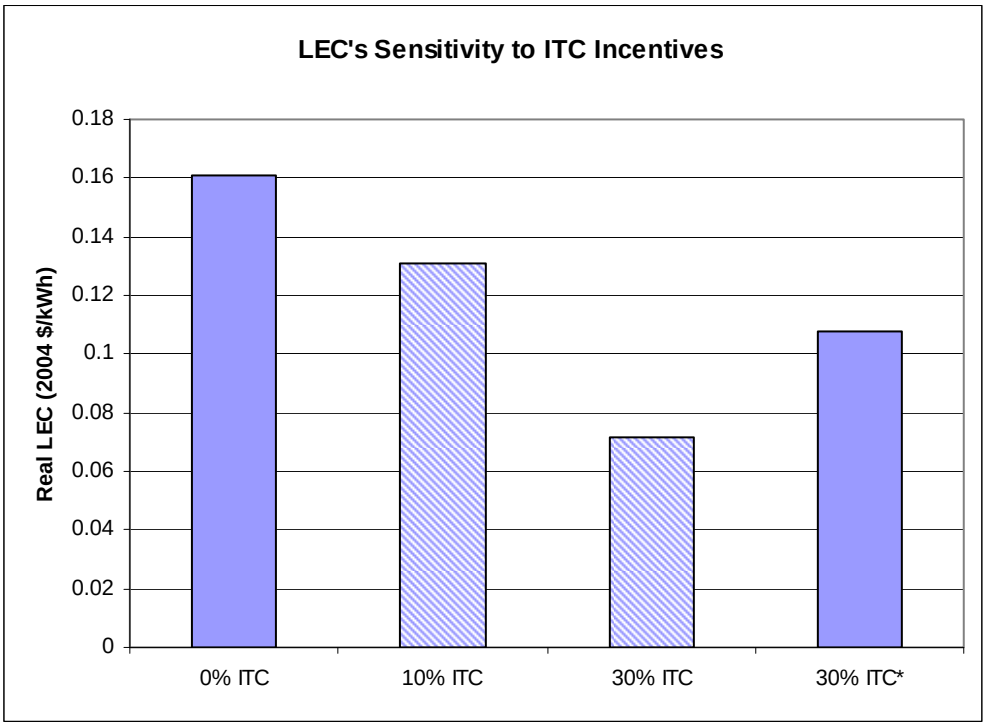

(3) Depreciation Method

Since solar projects are very capital intensive, the LEC can be very sensitive to the depreciation method used. If we use 15-year MACRS, the LEC will increase to $0.2015/kWh. It will increase further to $0.2616/kWh and 163% of the baseline if we assume 20-year MACRS. Table 2-5 and Figure 2-5 illustrate LEC's sensitivity to different MACRS schedules. We can see that the assumption of the MACRS schedule significantly changes the LEC result.

Table 2-5. LEC's Sensitivity to Depreciation Method

Sensitivity to Depreciation Method	**5-yr MACRS**	**15-yr MACRS**	**20-yr MACRS**
Real LEC (2004 $/kWh)	0.1608	0.2015	0.2616
Relative Cost Comparing to the Baseline	100%	125%	163%
MADSCR	1.53	2.02	2.74

Figure 2-5. LEC's Sensitivity to Depreciation Method

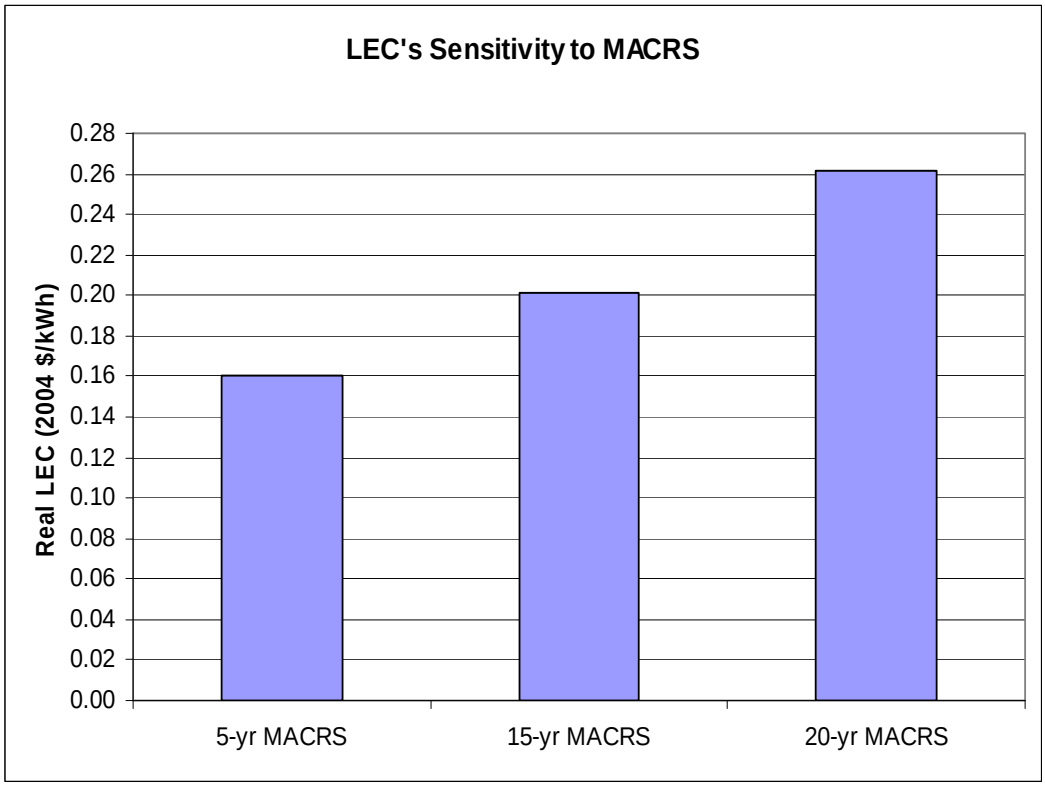

(4) Direct Normal Irradiance

DNI, depending on location and collection efficiency, can also significantly affect the CSP LEC. As shown in Table 2-6 and Figure 2-6, if DNI goes down to 6.05 kWh/m^2/day (e.g. Albuquerque, New Mexico), the LEC goes up to $0.1992/kWh and further up to $ 0.2306/kWh if DNI is 5.14 kWh/m^2/day (e.g. Austin, Texas).

Table 2-6. LEC's Sensitivity to Direct Normal Irradiance

Sensitivity to Direct Normal Irradiance (kWh/m^2/day)	**7.65 (San Diego/CA)**	**6.05 (Albuquerque/NM)**	**5.14 (Austin/TX)**
Real LEC (2004 $/kWh)	0.1608	0.1992	0.2306
Relative Cost Compared to San Diego (Baseline)	100%	124%	143%
MADSCR	1.53	1.53	1.53

* Direct Normal Irradiance is imputed based on NASA data.

Figure 2-6. LEC's Sensitivity to Direct Normal Irradiance

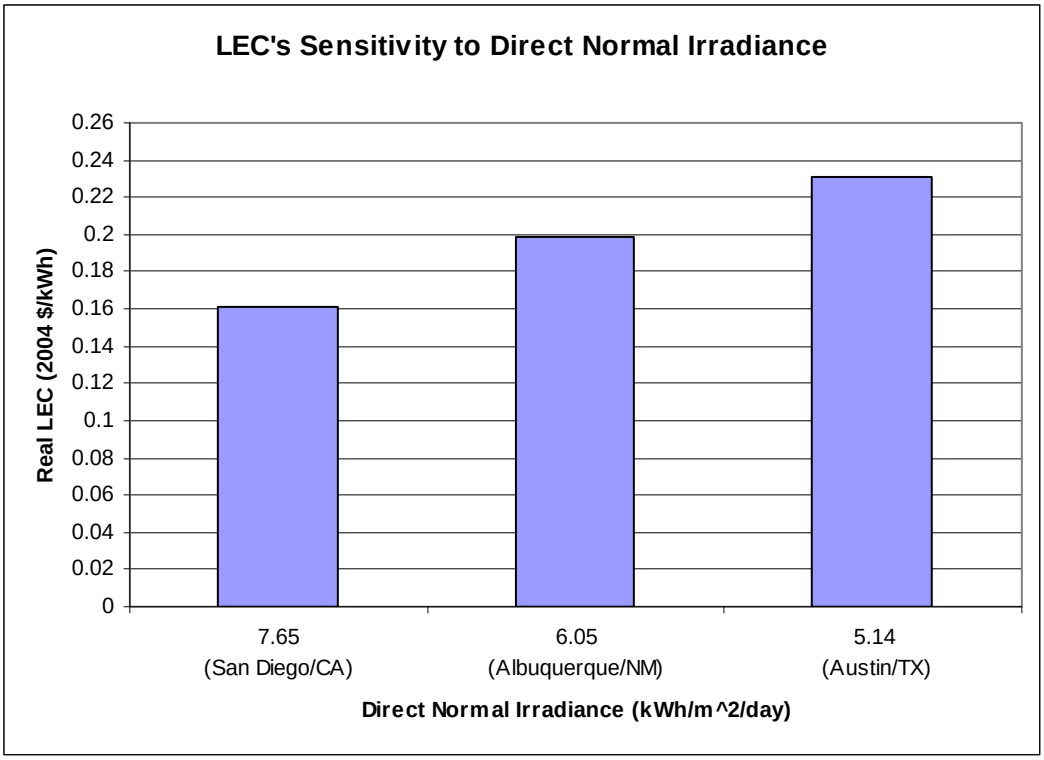

2.6 CSP LEC Calculation Using the Public Sector Economic Analysis

LEC from the public perspective can be calculated using the following formula

(2-3)

$$LEC = \frac{FCR * I + OM + F}{E}$$

Where

FCR = Fixed charge rate, a constant discount factor can be calculated using –PMT(discount rate, life time of the plant, 1)+ insurance rate.
I = Installed capital cost
OM = Annual operation and maintenance costs
F = Annual expenses for fuel
E = Annual energy production

This method is significantly simpler compared to the private financing cash flow model. The basic assumptions are the same as the ones in

Table 2-1 except for the discount rate. Because the public sector economic analysis ignores financing and tax effects, the major assumption that determines the LEC is the discount rate. As we discussed earlier, the social discount rate is usually smaller than the one used in the private financial analysis, so we assume 8% discount rate for the baseline. The calculated baseline LEC from the public perspective is $0.1535/kWh, is quite comparable to the baseline LEC from the private perspective. Table 2-7 and Figure 2-7 present the LEC's sensitivity to the discount rate. We can see that LEC is moderately sensitive to the discount rate.

Table 2-7. LEC's Sensitivity to Discount Rate: Public Perspective

	Discount Rate			
LEC's Sensitivity to Discount Rate	8%	6%	7%	9%
Fixed charge rate (FCR)	9.38%	7.76%	8.56%	10.23%
LEC from public perspective (2004$/KWh)	0.1535	0.1311	0.1421	0.1653
Relative Cost Comparing to the Baseline	100%	85%	93%	108%

Figure 2-7. LEC's Sensitivity to Discount Rate: Public Perspective

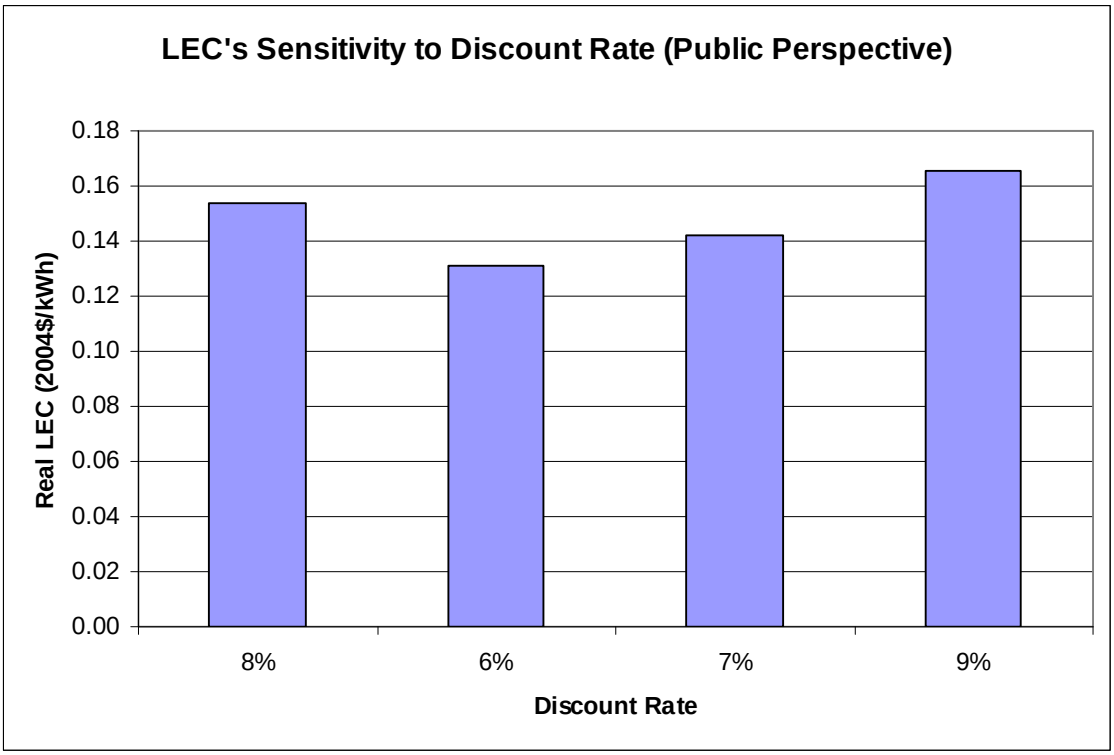

2.7 Conclusion

In this chapter, we document the methodologies of calculating LEC from both the private perspective and the public perspective. We find that LEC from the private perspective is very sensitive to financing assumptions, policy incentives, and levels of direct normal irradiance. The factors with the largest effect on LEC are investment tax credits, depreciation schedule, and direct normal irradiance.

In terms of financing assumptions, we examined how types of financing, debt-equity ratio, and interest rate affect LEC. We find that high debt-equity ratio without an increased interest rate can significantly decrease LEC. Holding other financing assumptions unchanged, interest rates only moderately affect LEC.

In terms of policy incentives, we examined the effect of investment tax credits and depreciation schedules. We find that either policy incentive can reduce LEC tremendously. Our baseline assumes current depreciation schedule (5-year MACRS) for solar energy. If this favorable policy is lifted, the estimated LEC can increase more than 60%.

Another caveat is that many lenders require certain minimum annual debt service coverage (MADSC), and we find that some lowest cost scenarios (e.g. municipal financing, 10% ITC and 30% ITC) are not able to meet this requirement without changing other assumptions such as special payment structures or other arrangements. Therefore, special attention should be given to these assumptions when comparing LECs between different analyses. Alternatively, the method of calculating LEC from the public perspective is much simpler. Comparable results can be obtained between the simple public method and the more detailed calculation given appropriate assumptions for the discount rate.

References

Board on Energy and Environmental Systems (BEES) (2002). Letter Report: Critique of the Sargent and Lundy Assessment of Concentrating Solar Power Cost and Performance Forecasts (2002).

http://books.nap.edu/openbook.php?record_id=10587&chapselect=yo&page=1

US 109 Congress (2005). Energy Policy Act of 2005 http://www.doi.gov/iepa/EnergyPolicyActof2005.pdf

Kearney, D and H. Price (2004) "Recent Advances in Parabolic Trough Solar Power Plant Technology." Manuscript from the authors.

Kistner, R., and H. Price, 1999, "Financing Solar Thermal Power Plants." Proceedings of the ASME Renewable and Advanced Energy Systems for the 21st Century Conference, April 11-14, 1999, Maui, Hawaii

National Renewable Energy Laboratory (2005) Potential for Renewable Energy in the San Diego Region, Appendix E, August 2005.

Price, H and S. Carpenter (1999) "The Potential for Low-Cost Concentrating Solar Power Systems." Conference Paper, NREL/CP-550-26649.

Price, H. (2006) "Concentrating Solar Power", Presentation to Global Energy Strategy Addressing Climate Change Technical Workshop. May 2006.

Sargent & Lundy LLC Consulting Group (2003) Assessment of Parabolic Trough and Power Tower Solar Technology Cost and Performance Forecasts. NREL/SR-550-34440. October 2003.

Short, W., Packey, D.J., Holt, T., 1995, "A Manual for the Economic Evaluation of Energy Efficiency and Renewable Energy Technologies", NREL/TP-462-5173, Golden, USA.

World Bank (1999) Cost Reduction Study for Solar Thermal Power Plants. May 1999.

3 Methodology for Estimating the CSP Electricity Cost: A New Approach for Modeling CSP Market Potential

3.1 Introduction

With higher energy costs and new regulatory support, concentrating solar power (CSP) technology, using the sun's thermal energy to generate electricity from steam, has re-emerged as a potentially competitive power generation option, particularly in arid regions where power demand peaks during the heat of the day. Currently over 45 CSP projects are in the planning stages globally with a combined capacity of 5,500 MW, according to Emerging Energy Research (2006), an advisory and consulting firm that tracks emerging technologies in global energy markets.

How competitive is CSP electricity and how much can CSP contribute to carbon reduction by replacing the traditional thermal power plants? The answers to these questions depend on the cost of electricity generated by CSP plants. Although a few studies (e.g. S&L, 2003, NREL, 2005) have projected future CSP costs based on certain assumptions such as technology advancement, economies of scale, and upward learning curves, few studies have considered the combined effects of intermittency, solar irradiance changes by season, system load changes over a year, and interactions with other generating units. Because the generation of a solar plant varies over the day and year, the interactions between CSP generators and other generators in the electric system may play an important role in determining costs. In effect, CSP electricity generation cost will depend on the CSP market penetration. This chapter examines this relationship.

Three different types of CSP technologies have been developed: (1) parabolic trough, (2) power tower, and (3) parabolic dish. There is significant design and cost variations among the three technologies. Because the parabolic trough is currently the most mature technology (Müller-Steinhagen and Trieb, 2004a), we focus on this technology and its characteristics in this chapter, although many of our insights could also apply to power tower technologies. The methodology we develop here is customized for the ObjECTS framework, but can also be adopted for other settings.

CSP plants either need backup auxiliary generation or storage capacity to maintain electricity supply when sunlight is low or not available. Therefore, the electricity generation cost for CSP plants has two components: costs arising from the solar component and costs due to the backup and/or storage components. All existing commercially operated CSP plants are hybrid plants. They either have a backup natural-

gas-fired boiler that can generate stream to run the turbine, or they have an auxiliary natural-gas-fired heater for the solar field fluid that can be used to produce electricity (NREL, 2005). This hybrid structure is an attractive feature of CSP compared to other solar technologies because the backup component has low capital cost and can mitigate intermittency issues to ensure system reliability. However, such hybrid CSPs are not cost effective to provide base load electricity. The addition of thermal storage would allow full use of available solar energy and would further reduce intermittency issues. A recent paper (Blair et al., 2006) that considers CSP's intermittency issue assumes six hours of thermal storage. As the paper indicates, this storage assumption greatly simplifies the treatment of resource variability. Because such a plant is assumed to be dispatchable, the capacity value for the plant is assumed to be equal to the capacity factor during the summer peak period. In addition, surplus is assumed to be negligible due to the general alignment of the solar resource and load. However, adding a 6-hour thermal storage to CSP plant can increase capital cost by more than 40% (NREL, 2005). Long-term cost effective thermal storage technologies are still under development. In this chapter, we focus on hybrid CSPs without storage and we will, therefore, deal with the intermittency issue directly. We will include the case with thermal storage in future research.

This chapter is organized as follows. Section II presents the detailed methodology and assumptions. To better illustrate the methodologies, we provide some example calculations. We present the results in Section III and conduct sensitivity analysis of key assumptions in Section IV. Then we conclude in Section V. For easy reference, Appendix 1 provides a detailed list of all variables used in this chapter.

3.2 Methodology and Assumptions

Three types of costs need to be considered to calculate the electricity generation cost of CSP plants: capital costs of building the CSP hybrid plant, variable costs of running the solar component, and variable costs of running the backup component. The capital costs for building the CSP plant are a function of plant capacity. To calculate variable costs, we need to know the electricity output from the solar component and from the backup component, respectively. Then the key questions are: When does the CSP backup mode need to run? How much electricity does the CSP backup mode need to generate? How will electricity output from the backup component and from the solar component depend on the market penetration level of CSPs? The following analysis addresses these questions.

Because the system load curve and the CSP electricity output are correlated and both are sensitive to time of the day and seasons, we first define our classification of time slices

and the system load curve. Secondly, because CSP electricity output from the solar component directly depends on solar irradiance levels, solar field size, and system efficiencies, we first discuss their quantitative relationships and then present how we process solar irradiance data in order to estimate CSP solar output. Finally, we detail our approach to estimating CSP output from the solar and the backup components separately for each time slice.

3.2.1 Classification of Time Slices

Since definition of seasons can vary by location, we define seasons based on irradiance levels as follows.

- Summer: the three months with the highest irradiance level.
- Winter: the three months with the lowest irradiance level.
- Spring/Fall: other months.

We then classify peak and intermediate load periods into different time slices for each season. The classification used is presented in Table 3-1. The exact definition of the time slices is for computational convenience and is not critical for the results other than a requirement that the summer peak should be identifiable as this is a key time period.

Table 3-1. Classification of Time Slices and System Load

Slice *i*	**Classification of Time Slices**	**Average System Load as A Percentage of the Maximum System Load**
1	Summer morning (5:00-5:30)	45.46%
2	Summer daytime 1 (5:30-9:00)	57.87%
3	Summer daytime 2 (9:00-14:00)	85.73%
4	Summer peak (14:00-17:00)	96.78%
5	Summer evening (17:00-24:00)	76.70%
6	Winter morning (6:00-10:00)	70.14%
7	Winter daytime (10:00-17:30)	63.85%
8	Winter evening (17:30-23:00)	67.69%
9	Spring/Fall daytime (5:00-19:30)	61.99%
10	Spring/Fall evening (19:30-22:00)	59.36%

3.2.2 System Load Curve

Electric system load, usually measured in megawatts (MW), refers to the amount of electric power delivered or required at any specific point or points on a system. A system load curve shows the level of a load for each time period considered. The assumed system load curve, denoted as $AveSysLoad^{i}$, is estimated using California electricity data for 2003 (CEC 2005). The average system load in each time slice as a fraction of the maximum system load is shown in Table 3-1.

The load of an electric utility system is affected by many factors such as customer mix (e.g. residential, commercial and industrial), temperature, and equipment type and efficiency. For example, a hot summer can significantly increase the summer peak load due to the increased cooling demand. We will examine how the shape of the load curve impacts the results later in the chapter.

Electric system load can be classified as base load, peak load, and intermediate (I&P) load. Base load refers to the minimum amount of power that a utility must make available to its customers and I&P load refers to the demand that exceeds base load. Thus base load power plants do not follow the load curve and generally run at all times except for repairs or scheduled maintenance. I&P generation varies with the load curve. Power plants that provide I&P load, in aggregate, must follow the load curve. For this analysis we consider the case where CSP plants serve I&P load.

3.2.3 Factors that Determine CSP Solar Output

CSP solar output directly depends on solar irradiance levels (duration and intensity), solar field size, and system efficiencies. Their quantitative relationships can be expressed in the following equation[4].

(3-1)

$$Output\_Net = Output\_Gross*(1-Loss\_Parasitic)$$

$$=(1-Loss\_Parasitic)*Eff\_Turbine*Asf*(DNI*Eff\_OPT-Loss\_HCE-Loss\_SFP)/1{,}000{,}000W/MW,$$

where the meanings of each variable and reference values are given in Table 3-2.

Once the CSP plant is built, the solar field area and system efficiencies are fixed, so using equation (3-1), we can calculate how CSP solar output varies with solar irradiance level.

[4] This functional form is from the Solar Advisor Model (SAM) developed by NREL, in conjunction with Sandia National Laboratory and in partnership with the U.S. Department of Energy (reference: personal communication with SAM support staff).

The assumed solar filed area is based on the optimal solar multiple we calculate for our baseline case. The solar multiple is the ratio of the solar energy collected at the design point to the amount of solar energy required to generate the rated turbine gross power (NREL, 2005). Higher solar multiples increase CSP plant capacity factors but also increase capital cost. An optimization procedure is used to find out the solar multiple that achieves the lowest CSP electricity cost, which is 1.07 in our baseline case.

Table 3-2 List of Variables Related to CSP Solar Output

Variable	**Meaning**	**Value**	**Source**
Output_Net	Design Turbine Net Output (MW)	--	Calculated
Output_Gross	Design Turbine Gross Output (MW)	--	Calculated
Loss_Parasitic	Electric Parasitic Loss (%)	11.1%	Assumed*
Eff_Turbine	Design Turbine Gross Efficiency (%)	36.4%	Assumed*
Asf	Solar Field Area (m^2)	685,666	Assumed***
DNI	Direct Normal Irradiance (W/m^2)	Value varies	§ 3.2.4
Eff_OPT	Optical Efficiency (%)	60.2%	Assumed*
Loss_HCE	HCE Thermal Losses (W/m^2)	42.629	Assumed**
Loss_SFP	Solar Field Piping Heat Losses (W/m^2)	10.05	Assumed **

References: *Kearney and Price (2004), ** SAM, *** Authors calculated optimal solar field area for a 100-MW net capacity CSP plant in Daggett Barstow, CA.

3.2.4 Solar Irradiance Data

We use solar irradiance data from NREL's National Solar Radiation Data Base 1961-1990 and 1991-2005 Update[5]. The 1991-2005 Update contains annual direct normal irradiance (DNI) hourly mean data and DNI threshold data (which indicate the number of subsequent days DNI is less than a certain threshold over the 15-year period). CSP plants require a minimum irradiance level to be operational. Currently, for plants without storage, the minimum irradiance level is assumed to be 300 W/m^2 (Kearney and Price, 2004). We use the DNI threshold data to calculate *NoSunDays*, which represents the number of days in a season during which there is not sufficient direct sunlight to operate the CSP plant. A threshold of 3000 Wh/m^2/day is used in this study. The threshold information is used to adjust the NREL's annual DNI hourly mean data to obtain an estimate of the DNI hourly mean value for each month for non-cloudy days, defined as days with irradiance greater than 3000 Wh/m^2/day.

We use Daggett Barstow (Lat (N) 34.87, Long (W) 116.78), California, as an example to illustrate the adjustment procedure as follows.

[5] Data source: http://rredc.nrel.gov/solar/old_data/nsrdb.

a. Obtain the 2005 annual hourly-mean DNI data for this location.[6] This is the average DNI for all days, including days when the CSP would not be operational due to low irradiance levels.
b. Obtain the monthly persistence report for this location.[7] There are several thresholds and we use the threshold of 3000 Wh/m^2/day. Since the calculations were performed for the entire 15-year period 1991-2005, we calculate the annual average number days lower than the threshold and then estimate the average daily DNI levels for those days. This calculation incorporates all the available threshold information so as to incorporate the fact that a threshold of 3000 Wh/m^2/day includes days with lower than 3000 Wh/m^2/day.
c. Impute the average daily DNI for each month and then the hourly DNI for those days less than the threshold, using the same monthly weight and hourly weight in data set (a). We assume that cloudy days have the same DNI distribution over each month as the 2005 annual hourly-mean DNI data, which includes both cloudy and clear days.
d. Adjust the hourly-mean DNI data from (a) to obtain hourly-mean DNI data for non-cloudy days by applying the following formula:
   (DNI_means*N_monthly-DNI_cloudy *N_cloudy)/(N_monthly-N_cloudy).
   Where DNI_means=hourly-mean DNI data in (a)
   DNI_cloudy=imputed cloudy-day hourly-mean DNI data in (c)
   N_monthly=number of days in that month
   N_cloudy=number of cloudy days in that month
e. Calculate the average non-cloudy day hourly-mean DNI for each season.

Figure 3-1 shows the adjusted hourly-mean DNI for non-cloudy days at Daggett Barstow by season. The reason we choose Daggett Barstow is that this location is close (around 30 miles) to Kramer Junction where several CSP plants have been built at and which is often used as a reference location in NREL reports. The adjusted annual daily DNI for non-cloudy days is 7.75 kWh/m2/day. In addition, as shown in Figure 3-1, although the highest hourly-mean DNI occurs in spring/fall, summer has the highest daily DNI and longest daylight hours.

3.2.5 Approximation of the Daily CSP Solar Output Profile

[6] Data source: http://rredc.nrel.gov/solar/old_data/nsrdb/1991-2005/statistics/hsf/723815_2005.hsf

[7] Data source: http://rredc.nrel.gov/solar/old_data/nsrdb/1991-2005/statistics/thr/723815.thr

Using equation (3-1), we find that the CSP solar output profile closely follows the solar irradiance curve. Therefore, we can use the solar irradiance curve to approximate the daily CSP solar output profile.

For simplicity, we idealize daily solar irradiance curve as an isosceles trapezoid symmetrically around the solar noon, as illustrated in Figure 3-2. The height of the trapezoid is the maximum irradiance during the day denoted as $MaxIrradiance$. The lower base and upper base of the trapezoid are the daylight hours (denoted as $Hour_{daylight}$) and noon hours (denoted as $Hour_{noon}$), respectively. The average daily irradiance (kWh/m^2/day) denoted as $DailyIrradiance$ is the area of ABFE.

Figure 3-1. Daggett Barstow Hourly-Mean DNI for non-cloudy Days by Season, 2005

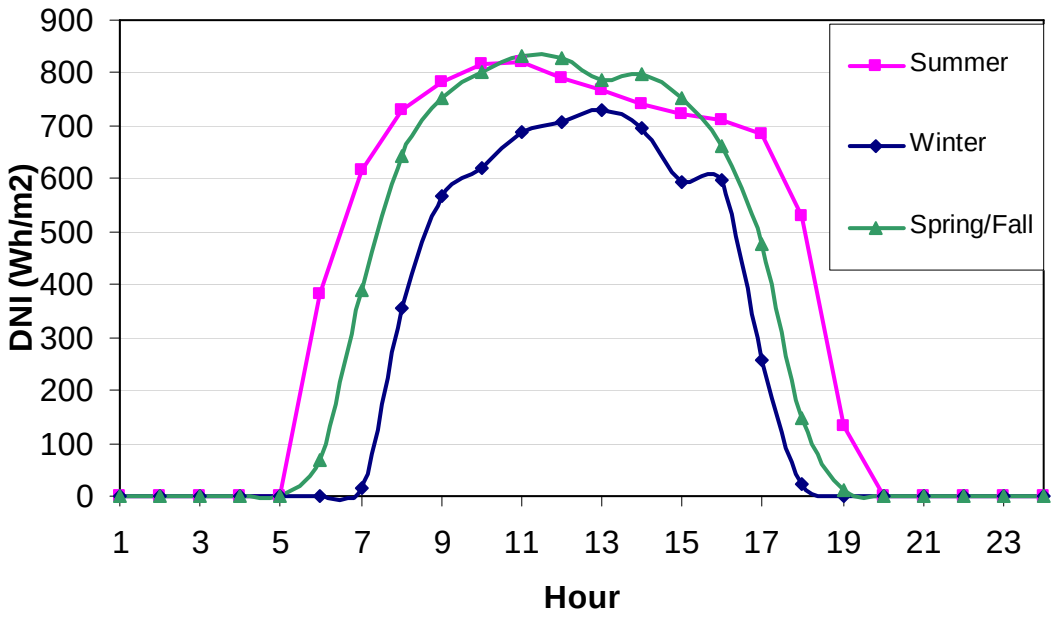

Figure 3-2. Solar Irradiance Curve by Time of the Day (Not to Scale)

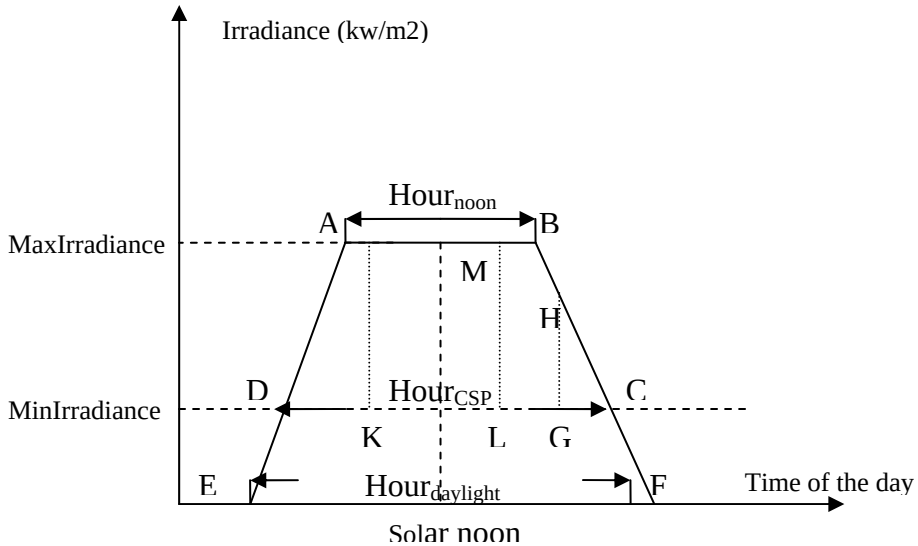

Given the average daily irradiance, noon hours, and daylight hours, we can obtain the maximum irradiance level in the day using the geometry of an isosceles trapezoid. We use solar irradiance data described above and get the least-square fit to the hourly- mean DNI data by varying noon hours. Once we know noon hours and the maximum irradiance level, we can calculate the daily CSP operational time $Hour_{CSP}$, the line CD in Figure 3-2.

Table 3-3 provides an example calculation of key solar geometry parameters by season for Daggett Barstow. We have implicitly assumed that variances in solar radiation in sunny regions such as the U.S. southwest can be described by the combination of seasonal irradiance curves for non-cloudy days and the *NoSunDays* parameter.

Figure 3-3 shows how well an isosceles trapezoid approximates the non-cloudy day solar irradiance curve by season. Although a fairly good fit, the approximation slightly extends the noon hours and flattens the irradiance level during the noon hours, which means that the approximation will slightly underestimate the peak solar output and overestimate the solar output in late mornings and late afternoons.

Table 3-3 Example of Calculating the CSP Operational Time: Daggett Barstow

Average by Seasons	Summer	Winter	Spring/Fall
$Hour_{noon}$ (hour)	9.64	6.55	7.36
$Hour_{daylight}$ (hour)	14.00	10.62	12.33
DailyIrradiance (kWh/m2/day)	9.23	5.85	7.95
MinIrradiance (kW/m2)	0.30	0.30	0.30
MaxIrradiance (kW/m2)	0.78	0.68	0.81
$Hour_{CSP}$ (hour)	12.32	8.83	10.48
NoSunDays	2	21	15

Figure 3-3. Approximation of an isosceles trapezoid on the daily solar irradiance curve by season

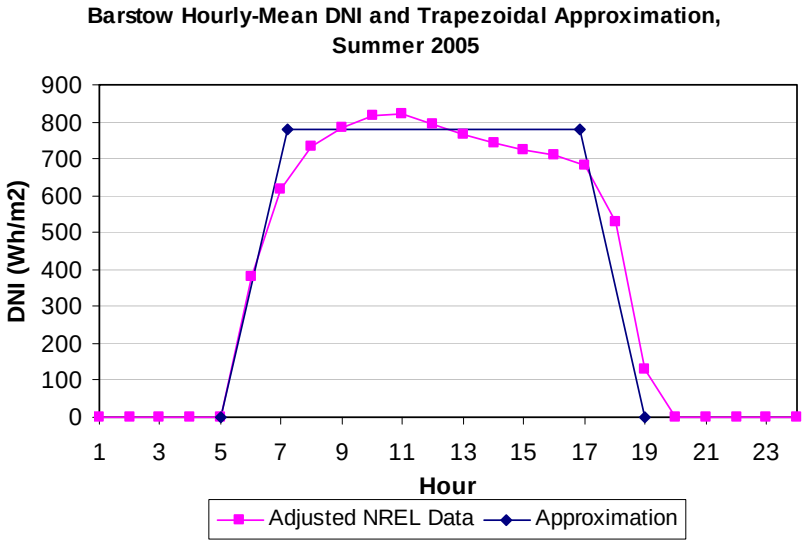
Barstow Hourly-Mean DNI and Trapezoidal Approximation, Summer 2005
DNI (Wh/m2)
900
800
700
600
500
400
300
200
100
0
1 3 5 7 9 11 13 15 17 19 21 23
Hour
Adjusted NREL Data
Approximation

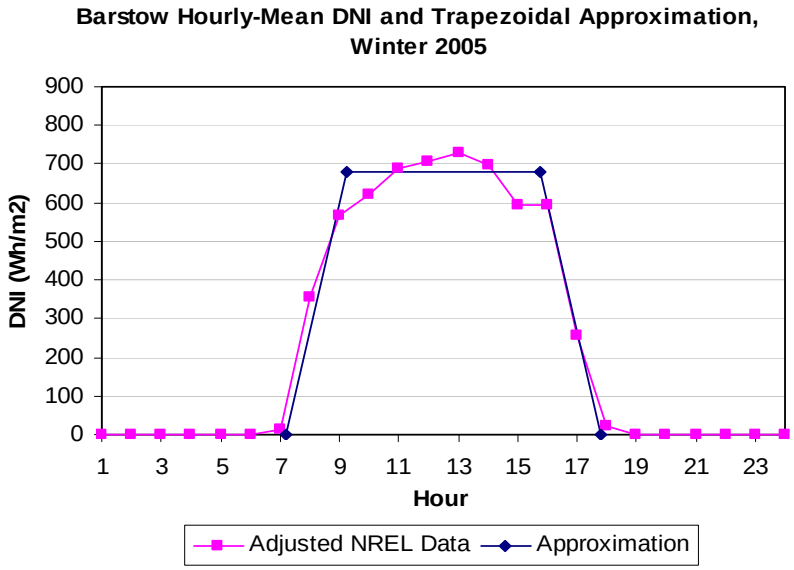
Barstow Hourly-Mean DNI and Trapezoidal Approximation, Winter 2005
DNI (Wh/m2)
900
800
700
600
500
400
300
200
100
0
1 3 5 7 9 11 13 15 17 19 21 23
Hour
Adjusted NREL Data
Approximation

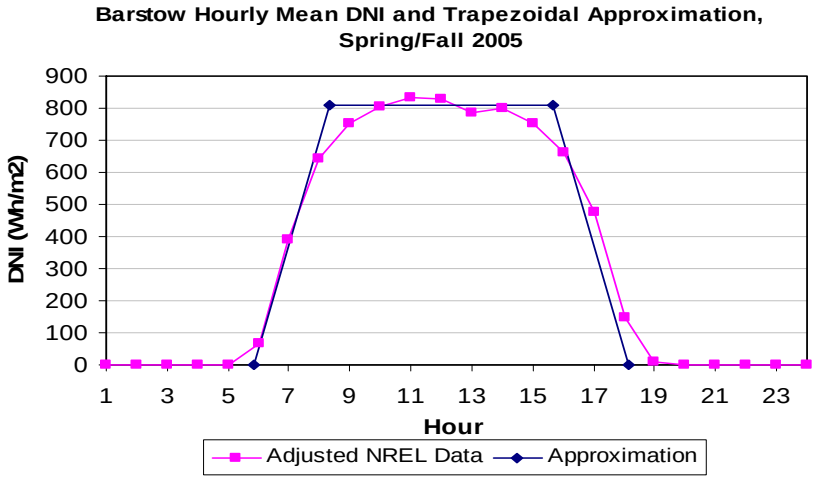
Barstow Hourly Mean DNI and Trapezoidal Approximation, Spring/Fall 2005
DNI (Wh/m2)
900
800
700
600
500
400
300
200
100
0
1 3 5 7 9 11 13 15 17 19 21 23
Hour
Adjusted NREL Data
Approximation

3.2.6 Electricity Output from the CSP Solar Component

Electricity output from the CSP solar component is determined not only by the irradiance level, but also by CSP market penetration. We define CSP market penetration (denoted as $MarketShare_{CSP}$) as the ratio of CSP output to the total output from the I&P load plants. The CSP output includes the output from the solar component (denoted as $CSPOutput_{solar}$) and from the backup component (denoted as $CSPOutput_{backup}$). These relationships are expressed in equations (3-2) and (3-3).

(3-2) $$CSPOutput = CSPOutput_{backup} + CSPOutput_{solar}$$

(3-3) $$MarketShare_{CSP} = CSPOutput / TotalOutput_{I\&P}$$

We first determine the potential CSP solar output, which varies by season depending on the solar resource, and then calculate the actual CSP solar output ($CSPOutput_{solar}$) which is determined by system demand for a given time slice.

- **Potential CSP Solar Output**

As we discussed earlier, the potential CSP output from the solar component (denoted as $PotCSPOutput_{solar}$) for each time slice depends on the solar irradiance level for that time slice, solar field area, and the system efficiencies. We use the solar irradiance curve to approximate the potential CSP solar output profile. Thus, through normalization, the potential CSP daily output can be measured as the area of ABCD in Figure 3-2. In order to calculate the potential CSP output for each time slice, we need to know the average hourly CSP output (denoted as $HourlyCSPOutput^{i}_{slar}$) and the CSP operational time (denoted as $Hour^{i}_{CSP}$) for each time slice, as shown in equation (3-4).

(3-4) $$PotCSPOupu\ t^{i}_{solar} = HourlyCSPO\ utput^{i}_{slar} * Hour^{i}_{CSP},\ \forall\ i$$

We have defined the time slices in such a way that for certain time slices CSP will not be operational. These times include summer morning, winter evening, and spring and fall evening. We calculate the potential CSP output for the remaining time slices. For example, as shown in Figure 3-2, the potential CSP solar output for four summer time slices *i*=2, 3, 4, 5 can be measured as the areas of ADK, AKLM, MLGHB, and HGC, respectively. The corresponding CSP operational hours are the lengths of DK, KL, LG, and GC. We implicitly assume that the irradiance level has dropped below the maximum irradiance level when evening time starts. Exceptions may be high latitude areas (e.g.

Norway). However, because CSP is not suitable in those areas due to the low annual average irradiance, those exceptions can be neglected.

To assess CSP solar generation capability by time slice, we define R^i as the ratio of average hourly CSP output for time slice *i* over the CSP summer maximum capacity (denoted as $Capacity_{CSP}^{summer}$) as shown in equation (3-5). $Capacity_{CSP}^{summer}$ is the maximum hourly output from the CSP hybrid plant in summer. Through normalization, $Capacity_{CSP}^{summer}$ is measured as the maximum irradiance level in summer.

(3-5) $$R^i = \frac{HourlyCSPOutput_{solar}^{i}}{Capacity_{CSP}^{summer}}, \ \forall i.$$

The variables R^i and $Hour_{CSP}^{i}$ are key results of this section. Since the normalized $PoCSPOutput_{solar}^{i}$ does not involve solar field area and system efficiencies, the calculations of the variables R^i and $Hour_{CSP}^{i}$ can be done at initialization once the solar irradiance data is available. Then $PoCSPOutput_{solar}^{i}$ can be calculated as shown in equation (3-6) using these two variables and the rated capacity of CSP (denoted as $Capacity_{CSP}$). The results do not depend on demand/supply assumptions as long as $Capacity_{CSP}$ does not change. Note that $Capacity_{CSP}$ here is the maximum hourly output from the CSP hybrid plant, which is the same whether running on solar or gas.

(3-6) $$PoCSPOutput_{solar}^{i} = \begin{cases} R^i * Capacity_{CSP} * Hour_{CSP}^{i} & \text{if } R^i \le 1 \\ Capacity_{CSP} * Hour_{CSP}^{i} & \text{otherwise} \end{cases}$$

Table 3-4 presents the ratio *R*, the total number of hours (denoted as $Hour^i$), and CSP operational hours (denoted as $Hour_{CSP}^{i}$) for each time slice using Daggett Barstow data, together with the assumed average system load as a percentage of the maximum system load for each time slice (demoted as $AveSysLoad^{i}$) and for each CSP operational time period (denoted as $AveSysLoad_{CSP}^{i}$) for comparison. Although the solar output overlaps significantly with the system demand, the correlation is not perfect. The highest three *R* ratios occur during summer daytime 2, summer peak, and spring/fall daytime while the three highest $AveSysLoad_{CSP}^{i}$ occur during summer evening, summer peak, and summer daytime 2. Note that the optimal solar multiple in this case is 1.07, thus the *R* ratio can be greater than 100% for certain time slices. However, due to CSP generator's capacity limitation, the actual output for those time slices cannot be greater than the rated capacity, which means the excess solar output greater than the rated capacity would be wasted if there is no thermal storage.

Table 3-4. CSP Solar Output Capability and Operational Hours by Time Slice: Daggett Barstow with a Solar Multiple of 1.07

Slice i	Time Slices	$Hour^i$	$AveSysLoad^i$	R^i	$Hour^i_{CSP}$	$AveSysLoad^i_{CSP}$
1	Summer morning (5:00-5:30)	0.5	45.46%	0.0%	0.00	45.46%
2	Summer daytime 1 (5:30-9:00)	3.5	57.87%	92.7%	3.16	59.16%
3	Summer daytime 2 (9:00-14:00)	5.0	85.73%	106.7%	5.00	85.73%
4	Summer peak (14:00-17:00)	3.0	96.78%	106.4%	3.00	96.78%
5	Summer evening (17:00-24:00)	7.0	76.70%	93.8%	1.16	99.37%
6	Winter morning (6:00-10:00)	4.0	70.14%	77.6%	1.91	68.80%
7	Winter daytime (10:00-17:30)	7.5	63.85%	88.8%	6.91	63.53%
8	Winter evening (17:30-23:00)	5.5	67.69%	0.0%	0.00	67.69%
9	Spring/Fall daytime (5:00-19:30)	14.5	61.99%	100.0%	10.48	64.28%
10	Spring/Fall evening (19:30-22:00)	2.5	59.36%	0.0%	0.00	59.36%

- **Actual CSP Solar Output**

The realized output from the CSP solar component is different from the potential output because the potential solar output can exceed the I&P load demand for certain periods. To calculate the actual electricity output from the CSP solar component, we need to take this into account. A similar issue with respect to the large-scale deployment of PV is discussed in detail in Denholm and Margolis (2006). Storage technologies such as integrated CSP thermal storage or stand-alone external storage can mitigate this loss. The analysis here considers CSP technologies without storage. Thermal storage will be considered in future work.

Since CSP plants in this paper are defined as I&P load power plants, we determine the I&P load demand for each time slice (denoted as $EDemand^i_{I\&P}$) using equation (3-6). Because some baseload capacity is often scheduled for maintenance in winter when electric demands are relatively low, we differentiate winter base capacity from non-winter base capacity in the calculation.

(3-6) $$EDemand^i_{I\&P} = (AveSysLoad^i - Capacity_{base}) * Hour^i, \forall i.$$

Similarly, we can calculate the intermediate and peak load demand for each CSP operational time slice, which is denoted as $EDemandCSP^{i}_{I\&P}$. Because supply must always equal demand, $EDemandCSP^{i}_{I\&P}$ is also the maximum output that CSP can produce for each CSP operational time slice (denoted as $MaxCSPOutput^{i}$). Any additional output that CSP produces will be lost. Therefore, the actual CSP output from the solar component for each time slice can be calculated as follows.

(3-7)

$$CSPOutput^{i}_{solar} = \begin{cases} PotCSPOutput^{i}_{solar} & \text{if } PotCSPOutput^{i} \le MaxCSPOutput^{i} \\ MaxCSPOutput^{i} & \text{otherwise} \end{cases}$$

where

(3-8)

$$\begin{aligned} MaxCSPOutput^{i} &= EDemandCSP^{i}_{I\&P} \\ &= (AveSysLoad^{i}_{CSP} - Capacity_{base}) * Hour^{i}_{CSP} \end{aligned}$$

$PotCSPOutput^{i}_{solar} - MaxCSPOutput^{i}$ is, therefore, the lost CSP solar output when $PotCSPOutput^{i}_{solar} > MaxCSPOutput^{i}$. We will discuss this term later.

In addition to scheduled maintenance which we assume usually happens during no/low sun days, solar fields may be forced to be out of operation due to some unforeseeable situation. We assume the forced outrage rate (denoted as *OutrageRate*) is 2% in this example. Thus, the annual CSP solar output is the sum of CSP output from all time slices considering the forced outrage rate, as shown in equation (3-9).

(3-9)

$$CSPOutput_{solar} = \sum_{i} CSPOutput^{i}_{solar} * N^{i} * (1 - OutrageRate)$$

where N^{i} denotes the number of non-cloudy days in a year for time slice *i*.

3.2.7 Electricity Output from the CSP Backup Component

Because the conversion efficiency of gas-to-electricity in hybrid CSPs is always lower than the efficiency of stand-alone gas turbines due to parasitic loads such as heaters and heat transfer fluid (HTF) pumps (NREL 2005, Leitner and Owens 2003), under optimal electric generation of the electric system, the backup mode would likely be used only after stand-alone gas turbines or other available capacity has been dispatched. Here we implicitly assumed that all other I&P load capacity not otherwise meeting load demand is

available for backup and will be fully dispatched before the CSP backup mode is dispatched. CSP backup generation would, therefore, likely be needed when the electricity output from the CSP solar component is low due to low irradiance, but electric demands remain relatively high and non-CSP capacity cannot meet demand, such as summer evenings. Although this optimal system efficiency should be achieved in the long term equilibrium under perfect competition, in reality, the system may operate in a non-optimal state due to coordination, transmission or contractual issues, which means that the backup mode may be dispatched before the stand-alone gas turbines or other more efficient available capacity. In that case, the electricity output from the backup mode will be greater than estimated in the following section. We return to this issue in Section IV.

Factors that affect the electricity output from the CSP backup component are the system load curve, irradiance level, and CSP market penetration level. The system load curve is important because ultimately the back-up mode is needed to meet electric demands after other cost-effective generators have been dispatched. Irradiance level by time of day and season is also directly relevant because it determines the electricity output from the CSP solar component. Finally, CSP market penetration level is our primary interest because it reflects how CSP would interact with other I&P load plant that are not affected by irradiance levels. In particular, we are interested in how the CSP cost changes as the CSP market penetration level changes.

For simplicity, we exclude the case that there is more than one type of CSP technology in the system. Under this assumption, once we know the actual CSP output from the solar component and the total intermediate and peak output, the calculation of CSP output from the backup component is straightforward. For each time slice, we first find out the corresponding I&P output requirement, and then compare this with the aggregated output level from the CSP solar component and non-CSP plants. If there is a deficit, the CSP backup mode will be dispatched to make up the deficit. The output using CSP backup mode is therefore

(3-10)

$$CSPOutput_{backup}^{i} = \begin{cases} EDemand_{I\&P}^{i} - CSPOutput_{solar}^{i} - Capacity_{nonCSP} * Hour^{i}, \\ \quad \text{if } EDemand_{I\&P}^{i} - CSPOutput_{solar}^{i} - Capacity_{nonCSP} * Hour^{i} \geq 0 \\ 0 \quad \text{otherwise} \end{cases}.$$

In addition, when CSP plants are not operational due to no/low sun days (lower than 300 W/m^2) or high wind days (greater than 35 mph), the CSP backup mode is needed to provide output for the CSP plant. Using data from NASA, we find that high wind days

are extremely rare, so we ignore this effect and only consider no/low sun day effects. We assume that the backup amount for each time slice is the corresponding average non-cloudy day CSP output. Thus, the annual output from the CSP backup mode due to no/low sun days can be calculated as follows.

$$CSPOutput_{backup}^{nosun} = \sum_i (CSPOutput_{solar}^i + CSPOutput_{backup}^i) * NoSunDays^i \quad (3\text{-}11)$$

where $NoSunDays^i$ denotes the number of no/low sun days in a year for time slice *i.*

Finally, the backup mode is needed when solar fields have forced outrage. The backup output for this part is

$$CSPOutput_{backup}^{outrage} = \sum_i CSPOutput_{solar}^i * N^i * OutrageRate \quad (3\text{-}12)$$

The total annual output from the CSP backup mode is the sum of backup output at each time slice due to solar supply deficit and the backup output due to no/low sun days and forced outrage.

(3-13)

$$CSPOutput_{backup} = \sum_i CSPOutput_{backup}^i * N_i + CSPOutput_{backup}^{nosun} + CSPOutput_{backup}^{outrage}$$

3.3 Results

Using the methods discussed above and using Daggett Barstow as an example, we calculate the fraction of backup mode operation and wasted solar output as a function of CSP market share, respectively. Finally, we present the calculated levelized CSP electricity cost.

3.3.1 Shares of Backup Operation and Solar Output Loss vs. CSP Market Penetration

Figure 3-4 shows how percentage of backup operation over the total CSP output and percentage of solar output loss over the total CSP output vary with CSP market penetration, respectively. When the CSP market penetration is less than 50%, the CSP backup mode is only used on no/low sun and forced outrage days, thus the backup share (denoted as S_{backup}) is constant at a low level. As the CSP market penetration increases,

the CSP backup mode is increasingly required for other occasions, starting from summer evenings and winter evenings in this example. When the CSP market penetration reaches 100%, S_{backup} increases up to 42%. The CSP solar output loss increases with CSP market penetration at a more rapid rate. When the CSP market penetration is less than 43%, there is only small CSP solar output loss due to the oversized solar field. After this threshold is passed, available solar output starts to exceed load demand, beginning with summer daytime 1 time slice. Thus, the share of CSP solar output loss increases rapidly and reaches nearly 50% when the CSP market penetration is 100%, which means that half of the total CSP output is wasted without storage.

Figure 3-4. Shares of Backup Operation and Solar Output Loss vs. CSP Market Penetration

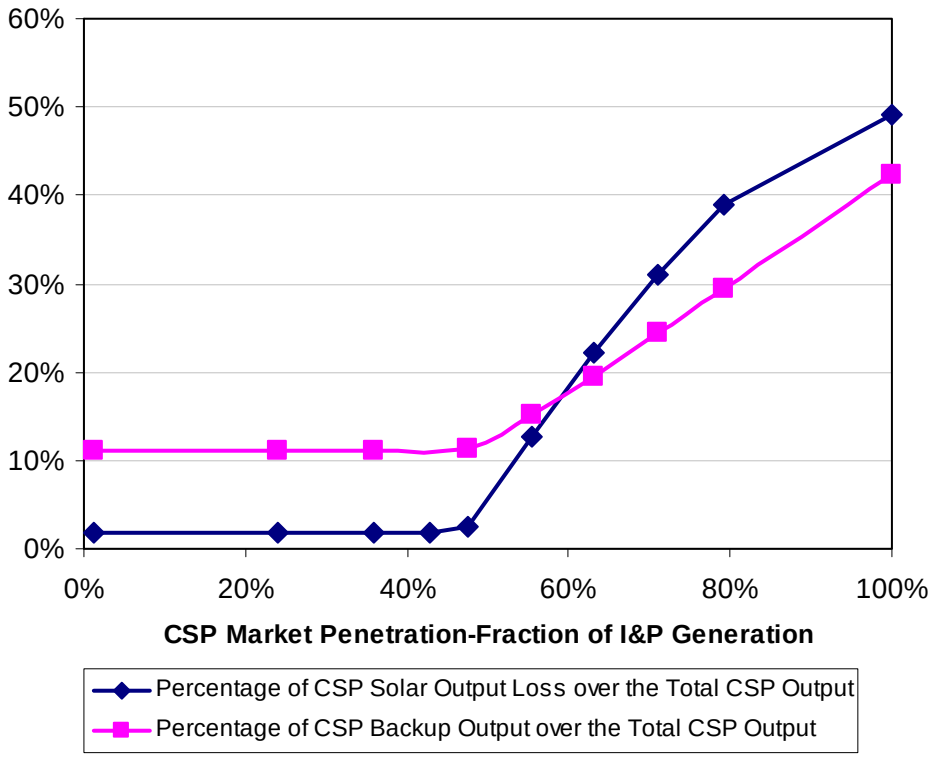

3.3.2 CSP Electricity Cost

One of the most useful measures of an electric generating technology is its levelized electricity generation cost (LEC). Using the methods discussed above, we can determine the annual CSP output from the solar and backup components for any given CSP capacity level. Then we can calculate variable costs of running the solar component and backup

components. In the following example, we calculate the levelized CSP electricity cost in Daggett Barstow using a simple public sector economic method discussed in chapter 2. This method provides comparable results with more sophisticated methods using private financial analysis, assuming various policy incentives such as 5-year modified accelerated cost recovery system (MARCS), but no investment tax credit (ITC). Because current policy incentives in the United States include both 5-year MARCS and 30% ITC for solar energy, the estimated baseline LEC in this paper is higher than one calculated assuming both policy incentives. We have not assumed the presence of ITC because we wish to consider the competitiveness of CSP technologies under a case where they have obtained a substantial market share, a situation where this type of additional policy incentives are less likely to be maintained.

Table 3-5 lists the baseline assumptions for the calculation. We first calculate fuel use and the total CSP output at each CSP market penetration and then use formula (3-14) to calculate levelized CSP electricity cost.

(3-14) $$LEC = \frac{FCR * I + OM + F}{CSPOutput}$$

Where FCR = Fixed charge rate, a constant discount factor can be calculated using –PMT(discount rate, life time of the plant, 1)+ insurance rate.
I = Installed capacity cost, which can be calculated as

$$I = c * Capactiy_{CSP}$$

where c=Capital cost per unit of installed CSP capacity.

OM = Annual operation and maintenance costs, which can be calculated as

$$OM = OM_{fixed} * Capactiy_{CSP} + OM_{\text{var}iable} * CSPOutput$$

F = Annual expenses for fuel, which can be calculated as

$$F = \text{Pr}ice_{gas} * (CSPOutput_{backup} / Efficiency_{gas-electricity})$$

where $Price_{gas}$ is price of fossil fuel natural gas.

As shown in

Figure 3-5, the levelized CSP electricity cost remains constant at $0.092/kWh until the CSP market penetration reaches 43%. It increases steadily to $0.122/kWh when the CSP market penetration reaches 100%. The levelized CSP electricity cost increases with CSP market penetration due to two factors, as shown in Figure 3-4, increased proportions of both wasted solar output and backup operation.

Because CSP market penetration is determined by the competitiveness of CSP electricity cost, the levelized CSP electricity cost in

Figure 3-5 refers to the equilibrium electricity market price. Since the levelized CSP electricity cost using the baseline assumptions is not yet competitive in the current electricity market, we include scenarios that the capital cost drops to 80% of the current level. When the capital cost drops to 80% of the current level, the levelized CSP electricity cost can be as low as $0.078/kWh, which is competitive with current I&P electricity prices. While it is impossible to predict future costs, U.S Energy Efficiency and Renewable Energy (EERE) program's Government Performance and Results Act (GPRA) of FY 2008, has projected costs that are in the range of our 80% reduction case by 2050 (EERE GPRA, 2007). We use this as the central case in the following sensitivity analysis.

Table 3-5. Baseline Assumptions for Calculating CSP LEC (in 2004$)

Variables	**Value**
Capital cost per unit of installed capacity assuming 1.07 solar multiple (*c*) ($/kW)	2801
Fixed O&M cost (OM_{fixed}) ($/kW-yr)	47.87
Variable O&M cost ($OM_{variable}$) ($/mWh)	2.72
Price of Fossil Fuel Natural Gas ($Price_{gas}$) (2004$/MMBtu) (HHV)	15.87
Gas to Electricity Conversion Efficiency ($Efficiency_{gas-electricity}$)	0.32
Lifetime of the plant (n)	30
Discount rate (*Rdiscount*)	8%
Insurance rate (*Rinsurance*)	0.5%

Figure 3-5. Levelized CSP Electricity Cost vs. CSP Market Penetration

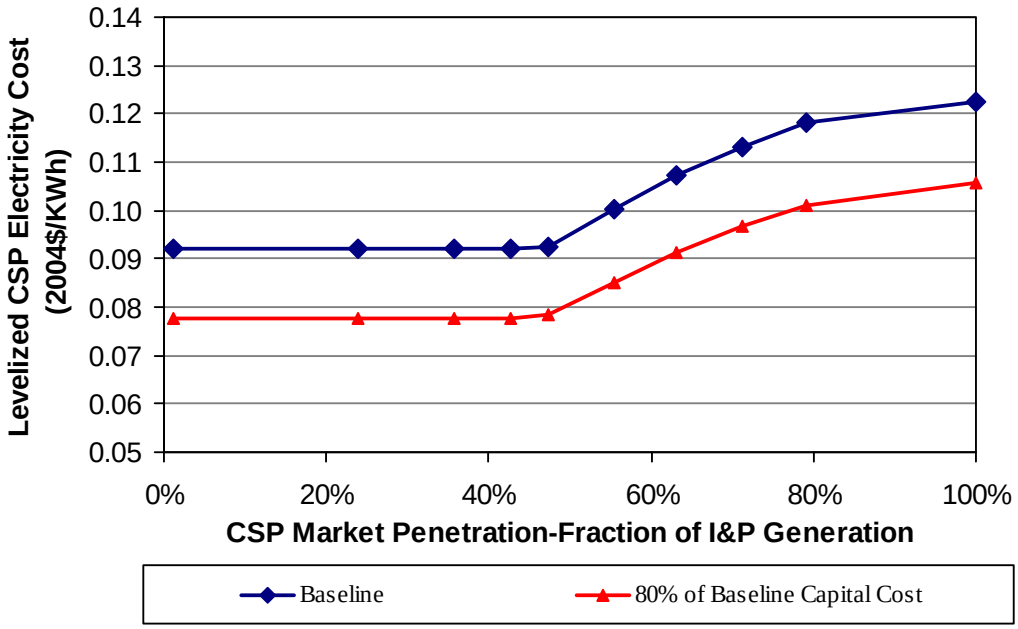

3.4 Sensitivity Analysis

In this section, we analyze the effects of carbon tax/gas price, system load curve, and system coordination and investigate how different assumptions on these key factors would change the results.

3.4.1 Effect of Carbon Tax/Gas Price

Because the share of CSP backup output increases with CSP market penetration, one concern is the effectiveness of using CSP to reduce carbon emissions. A carbon tax can be treated as an increase in gas price. To compare the impacts of carbon tax/gas price, Figure 3-6 presents a sensitivity analysis on gas price and its equivalent carbon tax. When a carbon tax $100/TC is used, the carbon tax causes an increase of LEC by $0.006/kWh in the extreme case of the 100% CSP market penetration and the impact of carbon tax is nearly negligible when CSP market penetration is low. The effect of a higher carbon tax of $500/TC is more prominent and can increase CSP levelized electricity cost by $0.008/kWh at the low market penetration and by more than $0.03/kWh at the 100% CSP market penetration.

In addition, we mark the LEC of stand-alone gas turbines at each corresponding gas price, respectively[8]. As shown in Figure 3-6, CSP is still competitive with stand-alone gas turbines when the CSP market penetration reaches the range of 70% to 80%.

Figure 3-6. Levelized CSP Electricity Cost vs. CSP Market Penetration- Sensitivity Analysis on Natural Gas Price/Carbon Tax

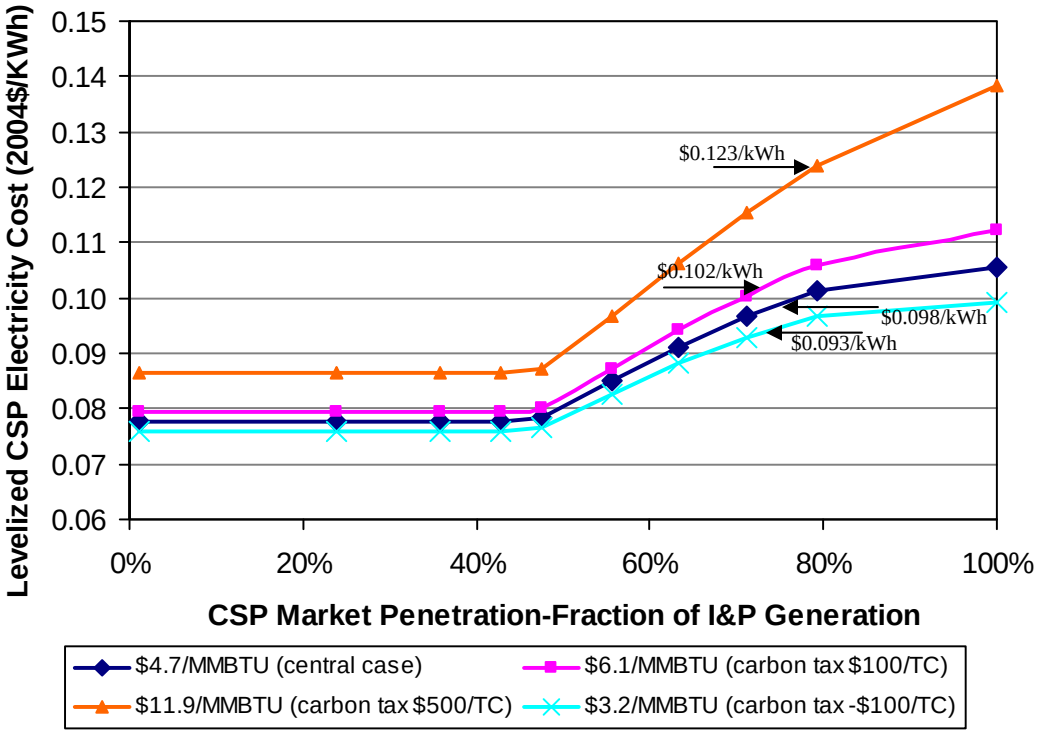

3.4.2 Effect of System Load Curve

Our baseline and central case assumptions use the estimated California system load curve. To understand how the shape of the system load curve may change our results, we conduct a sensitivity analysis. As shown in Table 3-6, using average system load as a percentage of the maximum system load by time slice as an indicator of system load curve, we consider three scenarios in addition to the central case: a region with hot summers, with cold winters, and with both hot summers and cold winters. When a region

[8] The capacity factor of stand-alone gas turbine for peak load electricity is assumed to be 0.1 and the capital cost is assumed to be 2004$ 392/kW. Reference is from the ObjECTS model.

has hot summers, it has a higher summer peak due to cooling demand, which causes smaller shares of load demand in winter and spring/fall since we always normalize the summer peak to 1. When a region has cold winters, it has a higher heating demand thus a larger share of load demand in winter. When a region has both hot summers and cold winters, this results in a smaller share of load demand in spring/fall.

Figure 3-7 presents the levelized CSP electricity cost for the system load curves scenarios. When CSP market penetration is less than 43%, there is no difference in LEC among different scenarios. However, when this threshold is passed, LEC in the scenarios with hot summers increases at a higher rate with CSP market penetration. This pattern is primary driven by changes in solar output loss as shown in

Figure 3-8. In the scenarios with hot summers, because the relative load in spring/fall is smaller, the available solar output starts to exceed the load demand during these periods even at moderate CSP market penetration levels. This means that levelized CSP electricity costs increase with CSP market penetration at a higher rate in the regions with hotter summers.

Table 3-6 Scenarios of System Load Curves

Slice *i*	**Classification of Time Slices**	**Average System Load as A Percentage of the Maximum System Load**			
		Central Case	Hot Summers	Cold Winters	Hot Summers & Cold Winters
1	Summer morning (5:00-5:30)	45.46%	42.66%	45.46%	42.66%
2	Summer daytime 1 (5:30-9:00)	57.87%	54.96%	57.87%	54.96%
3	Summer daytime 2 (9:00-14:00)	85.73%	84.72%	85.73%	84.72%
4	Summer peak (14:00-17:00)	96.78%	97.04%	96.78%	97.04%
5	Summer evening (17:00-24:00)	76.70%	75.35%	76.70%	75.35%
6	Winter morning (6:00-10:00)	70.14%	65.35%	71.92%	67.01%
7	Winter daytime (10:00-17:30)	63.85%	59.49%	64.68%	60.26%
8	Winter evening (17:30-23:00)	67.69%	63.07%	69.07%	64.35%
9	Spring/Fall daytime (5:00-19:30)	61.99%	57.75%	61.99%	57.75%
10	Spring/Fall evening (19:30-22:00)	59.36%	55.30%	59.36%	55.30%

Figure 3-7. Levelized CSP Electricity Cost vs. CSP Market Penetration by Scenarios of System Load Curves

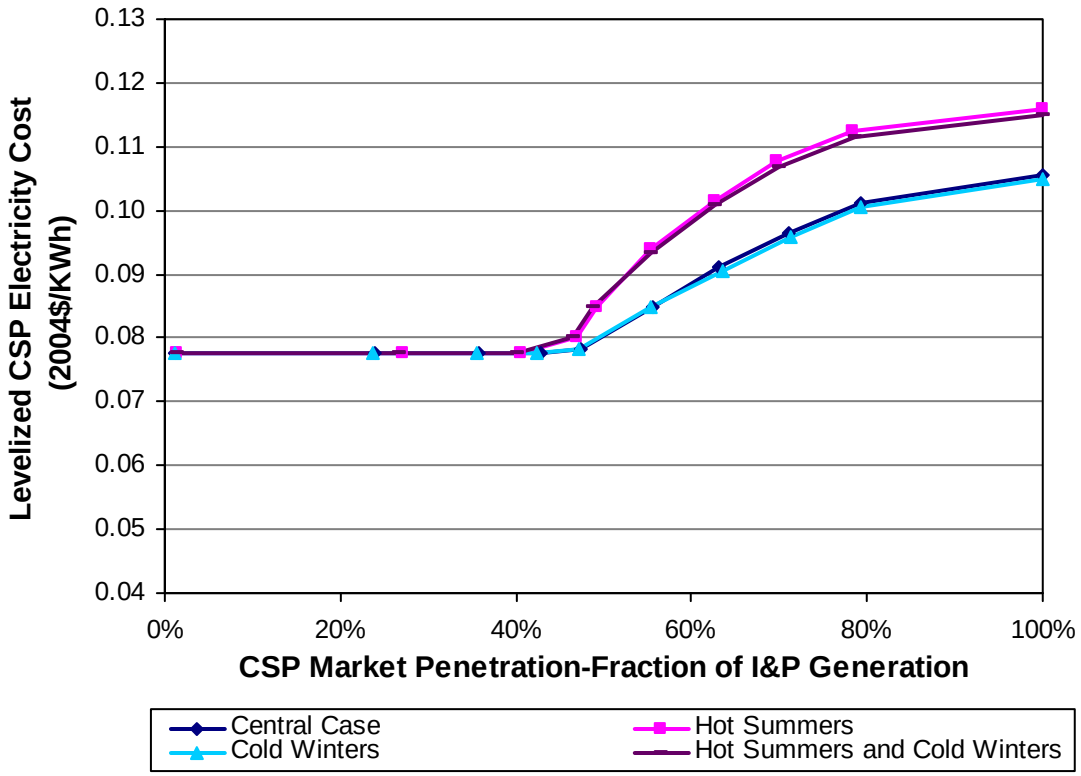

Figure 3-8. Percentage of CSP Output Loss vs. CSP Market Penetration by Scenarios of System Load Curves

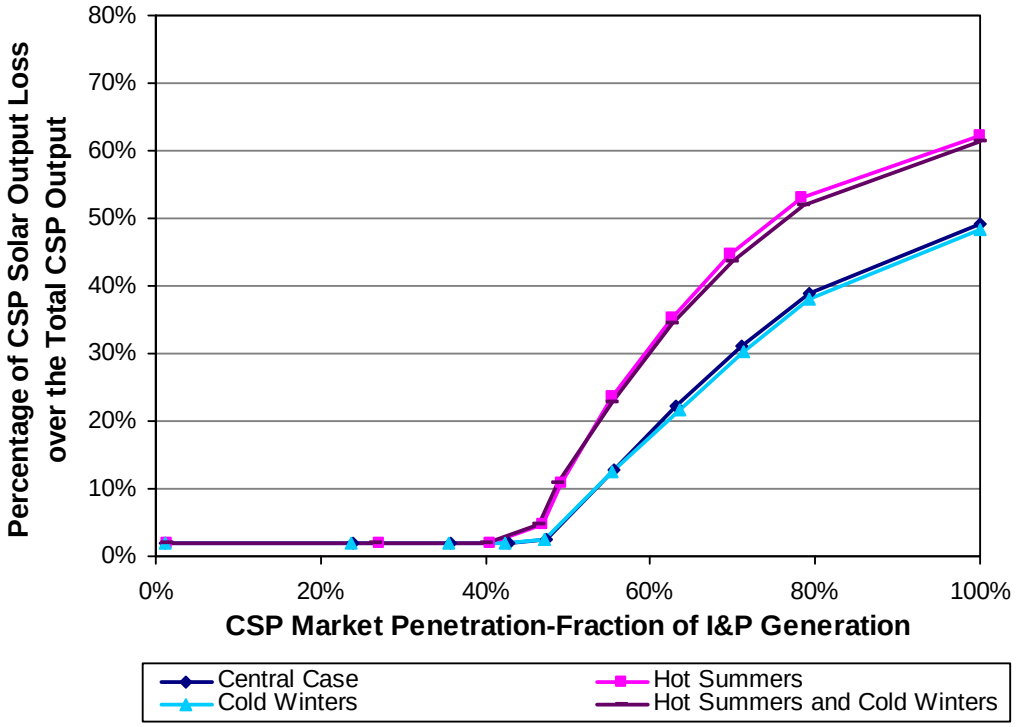

3.4.3 Effect of System Coordination

As we mentioned earlier, our analysis assumes that the electric system operates in an optimal state--more efficient available capacity such as stand-alone gas turbines will be dispatched before the CSP backup mode is used and solar output will be dispatched before other non-CSP I&P load supply. To ensure such an optimal state, additional costs due to coordination and contractual issues must be charged to CSP plants. If such an optimal state is not achieved and the CSP backup mode is dispatched before the stand-alone gas turbines or other more efficient available capacity, the electricity output from the backup mode will be greater than estimated here. Similarly, if non-CSP I&P load plants also operate when enough solar output is available, more solar output may be wasted. In the optimal state, as shown in

Figure 3-9, capacity factors of both CSP plants and non-CSP I&P load plants vary with CSP market penetration. The CSP capacity factor remains constant when CSP market penetration is below 50%. It then decreases with CSP market penetration and finally increases slightly when CSP market penetration reaches 100%. The capacity factor for non-CSP I&P technologies changes modestly when CSP market penetration is low and increases rapidly when CSP market penetration is over 80%.

We compare the optimal state with an extreme case of the constant non-CSP I&P capacity factor which means that capacity factor of non-CSP I&P load plants does not vary with CSP market penetration. Such case could be that non-CSP I&P load plants have long-term contracts with little flexibility and CSP plants are not treated differently from other non-CSP I&P plants. Capacity factors for CSP plants in this case are also constant with CSP market penetration. With the constant non-CSP I&P capacity factor, as shown in Figure 3-10, the levelized CSP electricity cost is higher than the system optimal state although the difference decreases with CSP market penetration and is even slightly lower than when the system is in an optimal state with a market penetration greater than 70%. The reason is mainly due to the fact that higher percentages of CSP output from the solar component is wasted when the CSP market penetration is low as non-CSP I&P output remains constant during the solar peak time. When CSP market penetration is high, although the total loss from the solar output is the same as the optimal state, the total CSP output in the constant non-CSP I&P capacity factor state is higher since more backup output is required. Therefore, the levelized CSP electricity cost is lower than the system' optimal state because of higher capacity factors when market penetration is high. These two states-the constant non-CSP I&P capacity factor state and the system optimal efficiency state-provide an upper and a lower bound for estimating the levelized CSP electricity cost as a function of the CSP market penetration.

Figure 3-9. Comparison of Capacity Factors for CSP and Non-CSP I&P Technologies

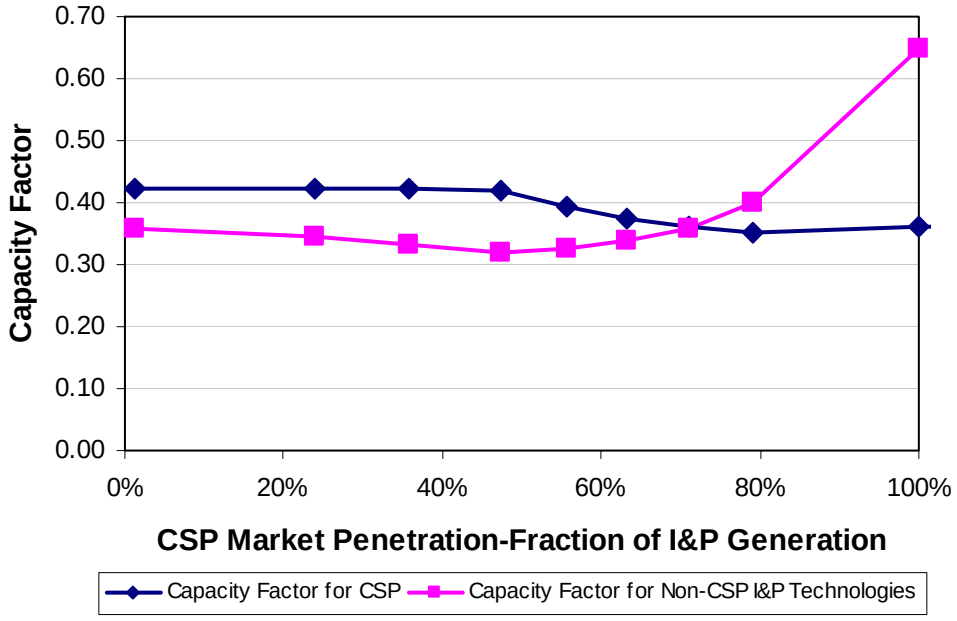

Figure 3-10. Levelized CSP Electricity Cost vs. CSP Market Penetration: the Case of Constant non-CSP I&P Capacity Factor

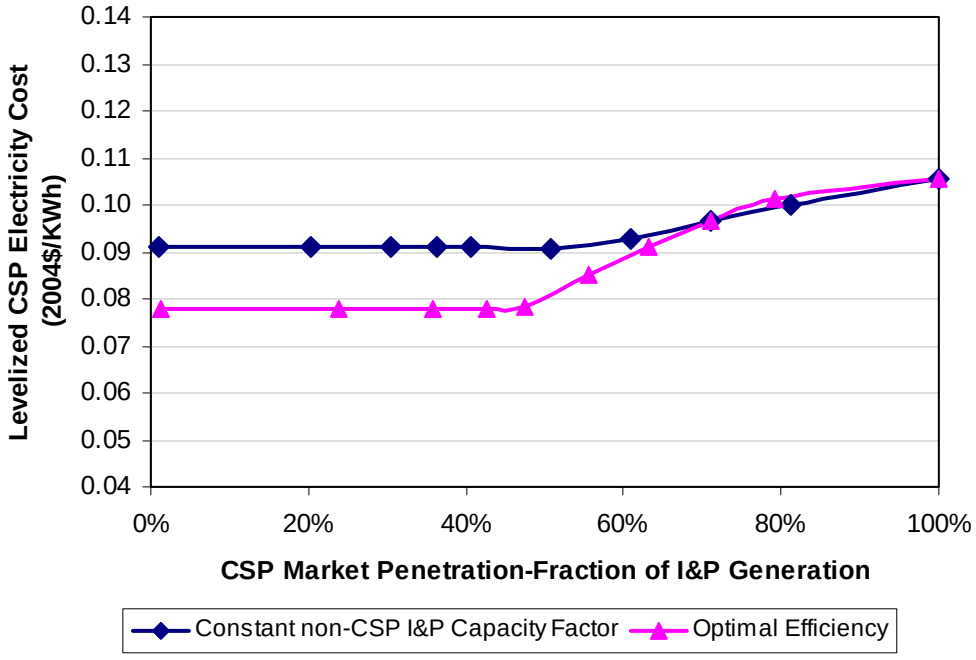

3.5 Conclusion

In this chapter we analyze how CSP electricity cost varies with CSP market penetration using current CSP technology with hybrid gas generation but without thermal storage. Using Daggett Barstow, CA as a sample site, we have shown that when CSP market penetration is less than 43% of the total I&P generation, the levelized CSP electricity cost does not depend on CSP market penetration. When the CSP market penetration is above the threshold, the levelized CSP electricity cost increases steadily with penetration. This is partly due to the increasing need for the backup output when the irradiance is low or unavailable and partly due the loss of CSP output from the solar component when there is excess supply (as shown in Figure 3-4). Because the CSP backup component is powered by fossil fuel, this means that when CSP market penetration level passes a certain threshold, the effectiveness of using CSP to reduce carbon emissions decreases. However, as shown in Figure 3-6, the effect of carbon tax on the levelized CSP cost is modest when the CSP market penetration is low. In addition, if the capital cost of the current CSP technology can be reduced by 20% as in the central case illustrated in Figure 3-6, the CSP market penetration could be competitive with natural gas turbines for penetration levels up to 70%. Therefore, CSP without thermal storage has potential to supply a large share of I&P generation without a significant penalty due to intermittency.

We focused on the CSP without thermal storage in this chapter. Trough designs can incorporate thermal storage to allow for electricity generation several hours into the evening and to increase the annual capacity factor. However, as we mentioned earlier, due to considerations of cost and some technical difficulties, all current commercially operated parabolic trough plants are hybrids without thermal storage. The SEGS I plant initially had 3-hours of thermal energy storage, but the system was damaged in a fire in 1999 (Kearney and Price, 2004). A couple of trough plants are being developed in Spain include 6-9 hours of thermal storage. However, they are research demonstration projects with governance support. In the case of CSP with storage, the issue of solar intermittency can be further mitigated. The loss of output from the solar component in the earlier discussion can be stored in this case. The minimum irradiance requirement can also be relaxed. Currently, for CSP without storage, a minimum irradiance level of 300 W/m^2 ($0.3kW/m^2$) is required to be operational. With storage, this solar energy can be stored and then used in the early evening when electric demand is still high. Thus we expect a higher share of output from the solar component. The potential of using thermal storage will depend on the tradeoff between the incremental cost of the storage system and the increased generation capacity factor. As we have shown in this chapter, the hybrid CSP solves intermittency quite well before CSP reaches 43% I&P market penetration. So hybrid CSP may be the most cost-effective solution in the near term. If long-hour (e.g. 12

hours or more) storage is available, the CSP plants could be fully dispatchable as discussed in Blair et al (2006) and could potentially be used as a base load technology. We will explore the tradeoffs between thermal storage capacity, cost, and other CSP system parameters in order to examine possible evolutionary pathways for CSP technologies in future research.

References

Blair, N., Mehos, M., Short, W., and Heimiller, D (2006) "Concentrating Solar Deployment System (CSDS) -- A New Model for Estimating U.S. Concentrating Solar Power (CSP) Market Potential." *Proceedings of the Solar 2006 Conference*, 9-13 July 2006, Denver, Colorado.

Denholm, P. and R. Margolis (2006) "Very Large-Scale Deployment of Grid-Connected Solar Photovoltaics in the United States: Challenges and Opportunities" *Conference Paper, NREL/CP-620-39683*

CEC (2005). Personal Communication: CEC HELM model annual energy and peak load estimates by end-use. California Energy Commission, November 15, e-mail.

EERE (1997) *Renewable Energy Technology Characterizations.* Topical Report TR-109496, Energy Efficiency and Renewable Energy (EERE), U.S. Department of Energy. http://www1.eere.energy.gov/ba/pdfs/entire_document.pdf

EERE GPRA (2007) "Projected Benefits of Federal Energy Efficiency and Renewable Energy Programs: FY 2008 Budget Request, Appendix D – Solar Energy Technologies Program." *Technical Report NREL/TP-640-41347* March 2007. http://www1.eere.energy.gov/ba/pdfs/41347.pdf

Emerging Energy Research (2006) "Concentrated Solar Power Heats Up." *Emerging Energy Research Market Brief on Solar CSP*.

Enermodal Engineering Ltd. (1999) *Final report prepared for the World Bank: Cost Reduction Study for Solar Thermal Power Plants*. World Bank, Washington DC. http://www.p2pays.org/ref/18/17974.pdf

Kearney, D and H. Price (2004) "Recent Advances in Parabolic Trough Solar Power Plant Technology." Manuscript from the authors. An older version of the paper with the same name is available at *Journal of Solar Energy Engineering*, May 2002, Volume 124, Issue 2, pp. 109-125.

Leitner, A and B. Owens (2003) "Brigher than a Hundred Suns: Solar Power for the Southwest." NBEL subcontract report. NREL/SR-550-33233.

Müller-Steinhagen, H and F., Trieb (2004a) “Concentrating Solar Power: A Review of the Technology.” *Quarterly of the Royal Academy of Engineering (Ingenia)*, vol 18, February/March 2004, pp 43-50.

Müller-Steinhagen, H and F., Trieb (2004b) “Concentrating Solar Power for Sustainable Electricity Generation: Perspectives.” *Quarterly of the Royal Academy of Engineering (Ingenia)* vol 19, May/June 2004, pp 35-42.

National Renewable Energy Laboratory (NREL) (2005) Potential for Renewable Energy in the San Diego Region, Appendix E, August 2005.
http://www.renewablesg.org/docs/Web/AppendixE.pdf

Price, H and S. Carpenter (1999) “The Potential for Low-Cost Concentrating Solar Power Systems.” *Conference Paper, NREL/CP-550-26649.*

Quaschning, V. (2004) "Technical and economical system comparison of photovoltaic and concentrating solar thermal power systems depending on annual global irradiation." *Solar Energy*, Volume 77, Issue 2, Pages 171-178.

Quaschning, V.; Kistner, R.; and Ortmanns, W. (2002) "Influence of Direct Normal Irradiance Variation on the Optimal Parabolic Trough Field Size: A Problem Solved with Technical and Economical Simulations." *Journal of Solar Energy Engineering*, Volume 124, Issue 2, pp. 160-164.
http://scitation.aip.org/getpdf/servlet/GetPDFServlet?filetype=pdf&id=JSEEDO000124000002000160000001&idtype=cvips&prog=normal

Sargent & Lundy LLC Consulting Group (S&L) (2003) Assessment of Parabolic Trough and Power Tower Solar Technology Cost and Performance Forecasts. NREL/SR-550-34440. October 2003

Appendix 1 – List of Variables

Variables	**Meaning**	**Source**
CSP Variables		
S_{backup}	The share of the output from the CSP backup	Calculated
Y	S_{backup} points used to approximate the CSP market penetration and backup share curve	Calculated
$MarketShare_{CSP}$	CSP market share, the ratio of the CSP output and the total output from the intermediate and peak load plants.	Calculated
X	$MarketShare_{CSP}$ points used to approximate the CSP market penetration and backup share curve	Calculated
$CapacityShare_{CSP}$	Share of CSP capacity of the total intermediate and peak load capacity	This is a trial value and assumed to be known initially.
CSPOutput	Annual CSP output (KWh)	Calculated
$CSPOutput_{backup}$	Annual CSP output from the backup component (KWh)	Calculated
$CSPOutput_{solar}$	Annual CSP output from the solar component (KWh)	Calculated
$Hour_{CSP}$	CSP operational hours	Calculated
$PoDailyCSPOutput_{solar}$	The potential daily CSP output from the solar component (KWh)	Calculated
CSPArea	CSP solar collection area (m2)	Assumed
$Efficiency_{CSP}$	Solar-to-electricity conversion efficiency	Assumed
$PoCSPOutput_{solar}$	Potential CSP output from the solar component (KWh)	Calculated

$MaxCSPOutput^{i}$	The maximum output that CSP can produce for CSP operational time slice i (KWh).	Calculated
R	The percentage of average hourly CSP output from the solar component over the full CSP capacity	Calculated
$HourlyCSPOutput_{solar}$	Hourly CSP output from the solar component	Calculated
$CSPOutput_{backup}^{nosun}$	Annual CSP output from the backup component due to no/low sun days (KWh)	Calculated
$AveDailyCSPOutput$	Average daily CSP output from the solar component	Calculated
c	Capital cost per unit of installed capacity ($/KW)	Assumed
OM_{fixed}	Fixed O&M cost ($/MW)	Assumed
$OM_{variable}$	Variable O&M cost ($/MWh)	Assumed
$Price_{gas}$	Price of Fossil Fuel Natural Gas (2004$/MWh) (HHV)	Assumed
n	Lifetime of the plant	Assumed
Rdiscount	Discount rate	Assumed
Rinsurance	Insurance rate	Assumed
LEC	Levelized electricity cost for CSP	Calculated
Solar Variables		
$DailyIrradiance$	The average daily irradiance (KWh/m2/day)	NASA
$Hour_{noon}$	Hours with maximum irradiance	Assumed
$Hour_{daylight}$	Daylight hours	NASA
$MaxIrradiance$	Maximum irradiance of the day (KW/m2)	Calculated
$MinIrradiance$	Minimum irradiance that CSP can be operational (KW/m2)	Assumed
$NoSunDays$	Number of no/low sun days of a year	NASA

System Variables		
$AveSysLoad^{i}$	The average system load (MW)	Estimated from the ObjECTS model
$Capacity_{total}$	The system full supply capacity (equals to the summer peak load) (MW)	Estimated from the ObjECTS model
$Capacity_{I\&P}$	Intermediate and peak capacity (MW)	Estimated from the ObjECTS model
$Capacity_{CSP}$	Total CSP capacity (MW)	This is a trial value and assumed to be known initially.
$Capacity_{maintenance}$	Base load reduction for maintenance in winter	Assumed
$Capacity_{base}^{nonwinter} = Capacity_{total} - Capacity_{I\&P}$	Base load capacity in non winter seasons (MW)	Calculated
$Capacity_{base}^{winter} = Capacity_{total} - Capacity_{I\&P} - Capacity_{maintenance}$	Base load capacity in winter (MW)	Calculated
$Capacity_{nonCSP}^{nonwinter} = Capacity_{I\&P} - Capacity_{CSP}$	Total non-CSP intermediate and peak load capacity in non winter seasons (MW)	Calculated
$Capacity_{nonCSP}^{winter} = Capacity_{I\&P} - Capacity_{CSP} - Capacity_{maintenance}$	Total non-CSP intermediate and peak load capacity in winter (MW)	Calculated
$TotalOutput_{I\&P}$	The annual output for the intermediate and peak load demand	Calculated
$CapacityFactor_{I\&P}$	The average capacity factor of all intermediate and peak load technologies	Estimated from the ObjECTS model
$Output_{I\&P}^{i}$	The electricity output needed to meet the intermediate and peak load demand for time slice i (KWh).	Calculated
$EDemand_{I\&P}^{i}$.	The intermediate and peak load demand for time slice i (KWh).	Calculated
$EDemandCSP_{I\&P}^{i}$.	The intermediate and peak load demand for CSP operational time slice i (KWh).	Calculated

N_i	The number of days in a year for time slice i	Calculated

4 Impact of Intermittency of PV on System Reserve Margins

4.1 Introduction

Grid-connected PV systems will play an increasing role as PV technology advances and cost decreases. However, an important feature of PV systems is that the electric output depends on irradiance which is only available during daytime and can vary significantly from day to day. Unlike wind, solar output can be highly correlated over large areas. In the case of no/low sun days, the electric output from the PV systems over a large area could be very low or even zero. As the share of PV plants in an electric network increases, the reliability of the system decreases unless more reserve capacity is added to keep the required system reliable. This additional reserve capacity will raise the electricity cost from PV systems, which will be an important economic factor for PV's further penetration. In this chapter, we use the case of no/low sun days as an example to examine the impact of intermittency of PV on system reserve margins. Based on probability theory, we first develop a method to calculate reserve margin in the nominal system (i.e., without PV), then apply this method to calculate the impact of no/low sun days on additional system reserve margins for each stylized case. After the methodology section, we present some numerical examples and then conclude.

4.2 Assumptions and Methodology

(1) Nominal System

We begin with a nominal electric system without PV which contains *n* standard generation units (SGUs) each with capacity c, that together provide exactly the peak demand (*n*c*). Let us assume that each SGU has an independent failure probability *p* at any given time. Because interruptions in electric service can have large economic and social costs, the electric system is required to operate at a certain reliability rate. To ensure a reliability rate *R*, some reserve capacity *Cr* is required to ensure adequate generation at the peak-demand time. This required reserve capacity can be computed by first finding the probability distribution for the number of SGUs, denoted as *F*, that fail at the peak-demand time:

(4-1) $$P(F = f) = \binom{n}{f} p^f (1-p)^{n-f},\ f = 0,1,...,n.$$

We can thus compute the cumulative probability of having more than *f* failures:

(4-2)

$$P(F > f) = \sum_{i=f+1}^{n} \binom{n}{i} p^i (1-p)^{n-i},\ f = 0,1,...,n.$$

Letting *f** be the smallest f for which *P (F > f) < 1- R*, we see that *f** failure-free generators are needed to meet the reliability requirement, or in other words a reserve capacity *Cr = f*c* is needed. Reserve Margin is often defined as the amount of unused available capability of an electric power system (at peak load for a utility system) as a percentage of total capability. Therefore, the reserve margin in the nominal system can be calculated as follows:

(4-3) $$RM=f^*/n$$

(2) Increased Reserve Capacity upon Adding Generation

Now let us consider meeting an increase in peak load demand of *z*c* by adding *z* new PV generators each with capacity *c*. We assume that PV generators have the same features as SGUs during the peak-load time except for the impact of solar irradiance variation. This means that PV generators have the normal failure probability *p* independent of irradiance variation. We consider the following scenarios:

- Scenario A: PV as SGUs

  Here we assume that the peak-demand time is always on a sunny day, therefore, PV generators are the same as SGUs.

- Scenario B: Independent p_{ns}

  We assume that the probability of the peak-demand time in a no-sun day is p_{ns} and each added PV generator has an independent $p_{ns.}$ This means that the PV generators are geographically far enough that they are not affected by the same weather conditions. We estimate p_{ns} as the ratio of number of no sun days in the given year over 365.

- Scenario C: Joint p_{ns}

We assume p_{ns} is the joint probability of the peak-demand time in a no-sun day. This means that PV generators are geographically close enough that they are jointly affected by the same weather conditions.

- Scenario D: Joint p_{ns} with a Loss Factor

  Instead of assuming that PV generators will completely fail in a no-sun day as in previous cases, we assume that the PV generator capacity is reduced due to low-sun days. This could be interpreted as the case of cloudy days.

We discuss the methodology for calculating the impacts of no/low sun days on the additional system reserve margin for the four scenarios separately as follows.

Scenario A: PV as SGUs

In scenario A, adding *z* PV generators is equivalent to adding *z* SGU generators. When *z* SGU generators are added, the number F_{SGU} of failed generators at the peak-demand time is described by the following distribution:

(4-4) $$P(F_{SGU} = f) = \binom{n+z}{f} p^f (1-p)^{n+z-f},\ f = 0,1,...,n+z.$$

As always, we can thus find the cumulative probability of having more than f failures:

(4-5)

$$P(F_{SGU} > f) = \sum_{i=f+1}^{n+z} \binom{n+z}{i} p^i (1-p)^{n+z-i},\ f = 0,1,...,n+z.$$

Letting f^*_{SGU} equal the smallest *f* for which $P(F_{SGU} > f) < 1-R$, we obtain that f^*_{SGU} SGU generators are needed to meet the reliability requirement, or in other words a reserve capacity $f^*_{SGU} * c$ is needed. Thus, the additional reserve capacity that must be added is $(f^*_{SGU} - f^*) * c$. The additional system reserve margin is

(4-6) $$RM_{SGU} = (f^*_{SGU} - f^*)/z$$

Scenario B: Independent p_{ns}

Let us now find the additional reserve capacity needed when z PV generators with independent p_{ns} are added. To evaluate this amount, we find it convenient to first find the probability distributions for the numbers of SGUs F_S and PVs F_{PV} that fail at the peak-demand time:

(4-7)

$$P(Fs = f) = \binom{n}{f} p^f (1-p)^{n-f},\ f = 0,1,...,n.$$

(4-8)

$$P(F_{PV} = f) = \binom{z}{f} q^f (1-q)^{z-f},\ f = 0,1,...,z.$$

where q is the failure probability of PV generators, which is equal to (p+ $p_{NS)}$. We implicitly assume that the non-weather related failure rate for PV generators is the same as the SGU. We note that F_S and F_{PV} are independent, and further that the total number of failures F equals F_S + F_{PV}. We can thus obtain the probability distribution for F by convolving the distribution of F_S with that of F_{PV}:

(4-9) $$P(F = f) = P(F_S = f) * P(F_{PV} = f),\ f = 0,1,...n + z.$$

Then we can find the probability that F exceeds a threshold as

(4-10)

$$P(F > f) = \sum_{i=f+1}^{n+z} P(F = i)$$

Similarly, letting f^*_{PV} equal the smallest f for which $P\ (F > f) < 1 - R$, we obtain that f^*_{PV} generators are needed to meet the reliability requirement. The additional system reserve margin for scenario B is

(4-11) $$RM_{PV} = (f^*_{PV} - f^*)/\ z$$

Scenario C: Joint p_{ns}

Now we consider scenario C in which each PV generator has an independent normal failure probability plus a joint failure probability when a no-sun day occurs. In this case, the probability distribution for the numbers of PVs F_{PVJ} that fail at the peak-demand time

includes two parts. If the peak-demand time is in a sunny day, PV generator has a normal failure probability *p*. If it is in a no-sun day, all PV generators fail. Thus we can get

(4-12)

$$P(F_{PVJ} = f) = (1 - p_{NS})\binom{z}{f} p^f (1-p)^{z-f},\ f = 0,1,...z-1.$$

(4-13)

$$P(F_{PVJ} = z) = (1 - p_{NS})\, p^z + p_{NS}$$

Again, F_S and F_{PVJ} are independent, and further that the total number of failures F equals $F_S + F_{PVJ}$. Following the same equations in (4-9), (4-10), and (4-11), we can get the additional system reserve margin for scenario C.

Scenario D: Joint p_{ns} with a Loss Factor

The only difference between scenarios D and C is that the PV generator will not completely fail and instead it has a loss factor that reduces the electric output. We use *L* to represent percentage of loss of the full capacity due to low-sun days. Similar to Scenario C, the probability distribution of the numbers of PVs F_{PVL} that fail at the peak-demand time includes two parts: normal failure and reduced output failure due to low-sun days. If it is in a low-sun day, the total loss of PV capacity will be at least *L*z*c*. If all PV generators are operational during this low-sun day, the total loss of PV capacity will be *L*z*c*, but if *m (m>0)* PV generator fails during this low-sun day due to the normal failure probability, the total loss of PV capacity will be *(z-m)*L*c + m*c*, greater than *L*z*c*. This total loss of PV capacity is roughly equivalent to $c*f_{NS}$, where f_{NS} is the equivalent number of PVs that fail at the peak-demand time in a low-sun day and can be estimated as the following.

(4-14) $$f_{NS} = ceil\ ((z-m)*L) + m,\ f_{NS} >= z*L,\ m=0,1,\ldots,z$$

Ceil(X) is a function that returns the value of X upwards to the nearest integer.

Therefore, the probability distribution for the numbers of PVs F_{PVL} that are failed at the peak-demand time is

(4-15)

$$P(F_{PVL} = f) = (1 - p_{NS})\binom{z}{f} p^f (1-p)^{z-f},\ f = 0,1,..., f_{NS}-1.$$

(4-16)

$$P(F_{PVL} = f) = (1 - p_{NS})\binom{z}{f} p^f (1-p)^{z-f} + p_{NS}\binom{z}{m} p^m (1-p)^{z-m},\ f = f_{NS},...,z.$$

Then following the same equations in (4-9), (4-10), and (4-11), we can get the additional system reserve margin for scenario D.

4.3 Numerical Examples

We now give some numerical examples of the scenarios detailed above. We assume that the original electric system contains 100 SGUs and each SGU has a capacity *c* of 100 MW. The probability of failure *p* for each SGU is 8% and the required system reliability at the peak-demand time *R* is 99.9%. Following the method described above, we obtain the reserve margin for the nominal system *RM*=18%.

We then consider scenarios A, B, C, and D by adding *z* (*z*=1, 2, …, 100) new generators. We assume that the annual no/low sun days are 50 in scenarios B, C, and D (p_{NS}=50/365=13.7%) and in Scenario D the loss factor *L* due to low-sun day is 0.8. Using different scenarios Figure 4-1 shows the comparison of impacts of no/low sun days on additional system reserve margin.

As we expected, the additional system reserve margin requirement is lowest when it is always a sunny day (Scenario A), which is equivalent to the case of adding SGUs. The additional system reserve margin is required when the PV market penetration reaches 8% and then it fluctuates slightly around 11% as the PV market penetration increases. This reflects the additional reserve margin that would be needed for any new generation unit, a failure rate identical to the assumed SGUs.

The additional system reserve margin requirement is the second lowest when the extra failure rate for each PV-generator due to no-sun days is independent (Scenario B). The additional system reserve margin is required when the PV market penetration reaches 4% and then it fluctuates and approaches 28% as the PV market penetration increases. The large jump in required reserve capacity, from 11% to 28% is due to the fact that the probability of a no-sun day is larger than the assumed generic generator failure probability.

When no-sun or cloudy days are considered as joint failures over a large region (Scenarios C and D), additional system reserve margin is required when the PV market penetration reaches 3% and increases quickly as more PV-generators are added to the

system. Especially in the worst case that all PV-generators fail due to no-sun days (Scenario C), the additional system reserve margin requirement for PV systems converges to 100% (one-to-one back up) when the PV market penetration is over 40%. Similarly, in Scenario D when the loss factor is 0.8, the additional system reserve margin converges to 80%.

Figure 4-2 illustrates the impact of the number of no/low sun days on additional system reserve margin requirement. We consider a scenario similar to Scenario D above, with a loss factor of 0.8. We can see that the number of low-sun days matters most when the market penetration of PV is low. We also notice that the difference between 1 low-sun day and 50 low-sun days is much larger than the difference between 50 low-sun days and 100 low-sun days. As the market penetration of PV increases, the reserve margin converges to a constant value.

Figure 4-1. Impact of No/Low Sun Days on Additional System Reserve Margin by Different Scenarios

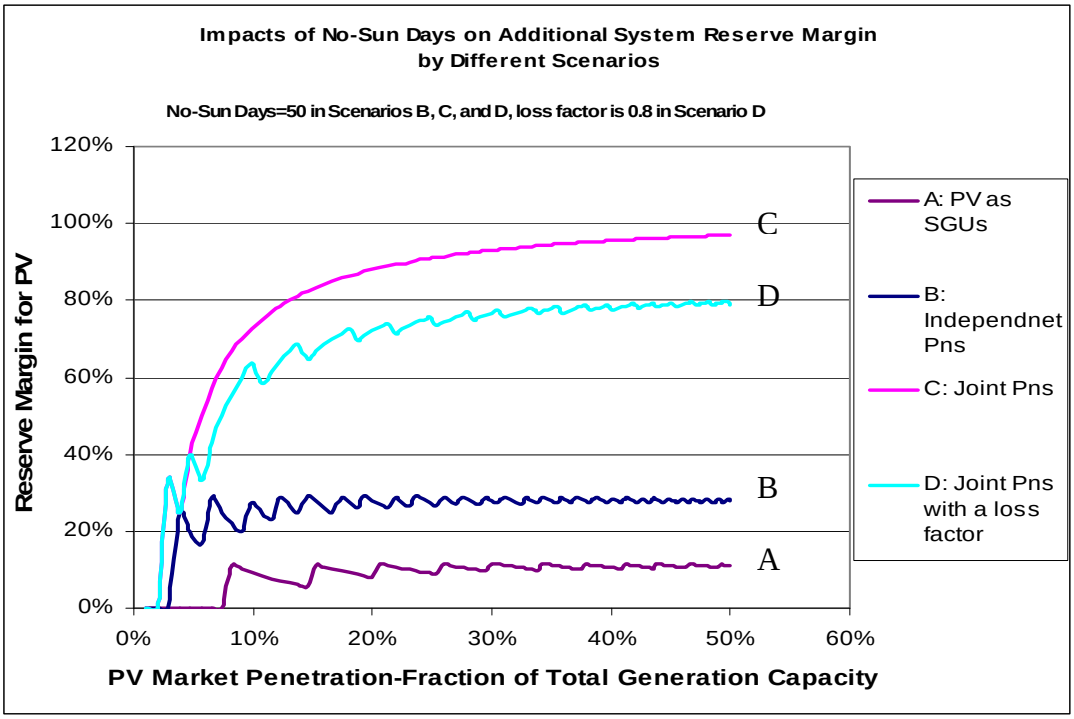

Figure 4-2. Impact of Number of No/Low Sun Days on Additional System Reserve Margin in Scenario D

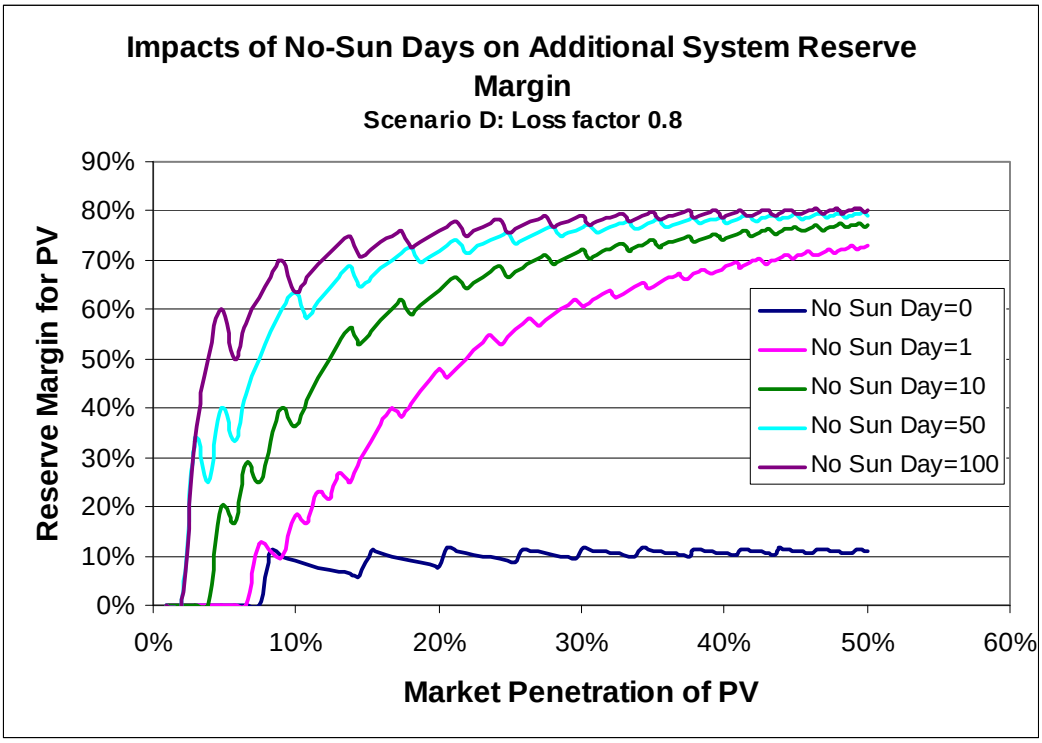

Figure 4-3. Correspondence Between Solar Irradiance and Temperature

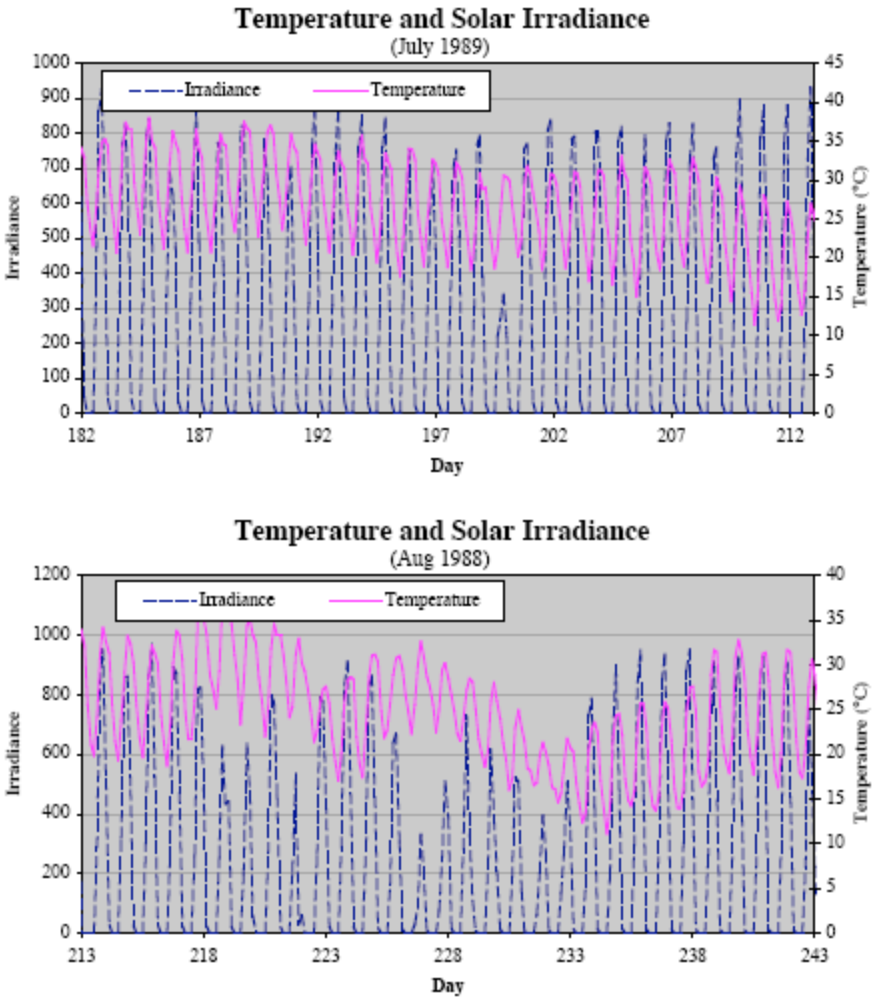

Two different months are shown. In July 1989, there was only one cloudy day (about day 200) where temperatures remained high. In August 1988, however, there were a number of days where temperatures remained high, but solar irradiance was small.
Source: NASA SEE (http://earth-www.larc.nasa.gov/solar/)

4.4 Conclusion

We analyzed the impacts of no/low sun days on PV reserve margin by exploring different scenarios in this chapter. This question is raised because it closely relates to PV electricity cost and how widely PV systems can be used. We find that the results can be

quite different depending on assumptions. When the market penetration of PV is low, the probability of having no/low sun days plays a particularly important role and therefore should be a consideration in addition to irradiance level when selecting the location for a PV system. When the market penetration of PV is high, the requirement for additional system reserve margin will increase dramatically (converge to one-to-one backup in the extreme case), which will significantly increase the PV electricity cost.

Although our analysis is based on stylized assumptions and uses simulated data, it provides a conceptual framework and indicative results on the impact of PV's intermittency feature. Analysis using the similar conceptual framework with more realistic spatial and temporal variable would be helpful.

Finally, we note that solar irradiance is often correlated with temperature, so also with electric demands, which could mitigate the requirement for additional system reserve margin caused by PV's intermittency. However, this correspondence cannot be guaranteed, as shown in Figure 4-3, which provides an example of daily irradiance and daily temperature, plotted every three hours for a location near Bakersfield California (Latitude: 35.5 N, Longitude 118.5 W) for July 1989 and August 1988. There is a significant correlation between temperature, and therefore cooling loads, and solar irradiance. There are, however, some days, and at times a series of days, where irradiance drops while temperature remains high. In July 1989 only one such day occurred. While this may be typical for this location, situations such as that illustrated for August 1988 may also occur where several cloudy, but otherwise hot, days occurred in sequence. On cloudy, hot days, the system would have to have alternative capacity in place to provide electricity that is not available from the PVs. This requirement may not be prohibitive in terms of cost, depending on the amount of PV capacity and the magnitude of the cooling demand, but it must be considered in system planning and analysis.

References

EERE (1997) *Renewable Energy Technology Characterizations.* Topical Report TR-109496, Energy Efficiency and Renewable Energy (EERE), U.S. Department of Energy. http://www1.eere.energy.gov/ba/pdfs/entire_document.pdf

Hogg, R. and Allen T. Craig (2004), *Introduction to Mathematical Statistics* (6th ed.), Prentice Hall.

5 The Role of Solar Energy Technologies: Preliminary Modeling in the ObjECTS Framework

5.1 Improved Representation of Solar Technologies

The work presented in the previous chapters was conducted to guide implementation of improved representations of solar energy technologies within the ObjECTS MiniCAM Framework. The previous representation of solar energy technologies was as one generic technology with a constant marginal cost that decreased over time, subject to a capacity constraint. This representation did not take into account resource quality or other aspects of specific solar technologies.

We have implemented an improved representation of solar technologies, focusing first on CSP technologies such as trough or power tower. The reason for the focus on CSP technologies is two-fold. First, in areas with good quality direct sunlight, CSP technologies that are currently less expensive than PV technologies are expected to remain this way for some decades. Further, since these types of CSP technologies are constructed with the option of hybrid mode operation, the electric system integration issues are minimized.

Our new representation of solar technologies is based on a more explicit description of both solar resources and solar technology characteristics. Solar resources are represented as km^2 of land with properties such as average irradiance and number of no-sun days. Any number of average irradiance values can be associated with each resource, for example, average direct irradiance for east-west tracking panels and average total irradiance. Any number of resource areas can be included. Each resource is represented as a function of distance to the electric grid so that the costs of connecting to the grid can be represented. The representation of solar resources within our modeling framework is similar to the new representation of U.S. wind resources (Kyle *et al.* 2007).

5.2 Preliminary Calculations of the Role of CSP power

CSP technologies are implemented using the representation developed in Chapter 3, which describes the amount of hybrid mode operation required as a function of market penetration of the CSP technology. As market penetration increases, the cost of energy increases as natural gas is consumed in hybrid mode operation and an increasing fraction of the available solar power is lost due to mismatches between load and demand (is load and demand the same thing? Maybe change to supply capacity and actual demand?).

An initial examination of CSP power was conducted by implementing CSP technologies into our current model version with an aggregate US electric market without time of day pricing. Initial CSP capital and operating costs, finance costs, and conversion efficiencies were derived from Kearney and Price (2005). For the reference case results shown in the next section, capital and operating costs were assumed to decline by 0.5% per year while efficiencies increased from 14% to 18% by the end of the century. For the advanced case, costs declined 1% per year while efficiencies increase to 22%. The assumed CSP capital costs are shown in Table 5-1. The costs in the advanced case are similar to those assumed for the EERE GRPA analysis program case (NREL 2007).

Solar resource data at a one-degree spatial resolution was obtained from the National Aeronautics and Space Administration (NASA) Surface meteorology and Solar Energy project.[9] Where the required type of solar resource data was not available from NASA, the closest available category was used and values were scaled by comparing point estimates from NREL and scaling the NASA data to match the NREL estimate. This provides a reasonable solar resource estimate for the current analysis, which focused on direct solar irradiance in high resource areas in the southwestern United States.

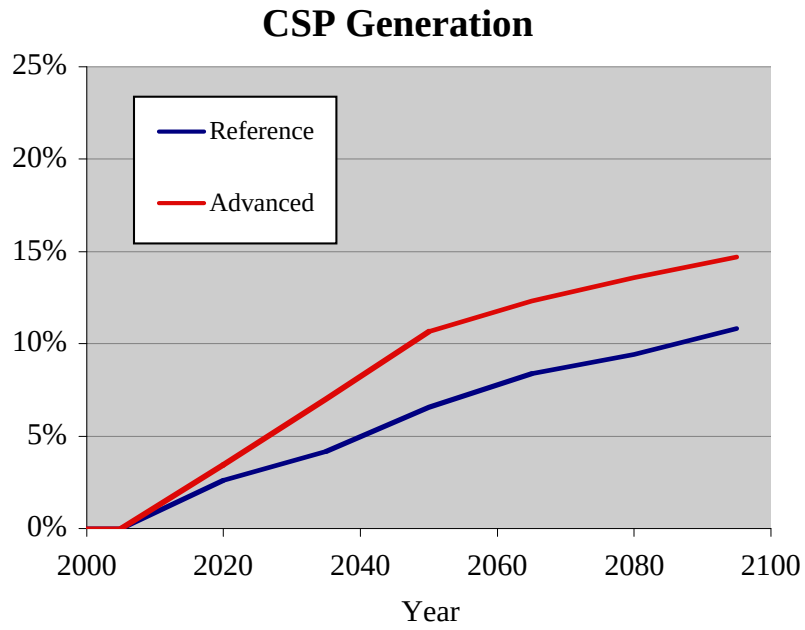

Figure 5-1. Thermal CSP penetration for reference and advanced case technologies. The penetration of CSP power is overestimated because geographic concentration of the solar resource was not taken into account (see text).

[9] See http://earth-www.larc.nasa.gov/solar/.

CSP capital costs ($2004/kWhr)

Year	Reference	Advanced
2005	2957	2957
2020	2265	2957
2035	2101	1985
2050	1949	1707
2065	1808	1468
2080	1677	1263
2095	1555	1086

Table 5-1. Assumed thermal CSP capital costs. No thermal storage was assumed.

The results of the model run are shown in Figure 5-1. We see that, if capital costs decline as projected, CSP technologies are capable of a significant contribution to U.S. electricity demand. The figures here are only for illustration, as the amount of intermediate and peak demand was not separately identified in this model run. This is necessary for a more accurate evaluation of CSP technologies and we will return to this point in the next section.

Because CSP operates only in the daytime, the relatively high penetrations in later years imply that a fraction of baseload capacity would need to be "turned-down" or reduced during the day in order to accommodate these high penetration levels. For example, see Denholm and Margolis (2006) for an analysis of PV technologies in this situation. The economics of this situation were not included in the current model result (but we considered the loss of CSP output?).

While the cost and, perhaps more importantly, the ability to connect resources to the electric power grid was a significant uncertainty for wind energy (Kyle *et al.* 2007), a sensitivity analysis found that this had little effect on the role of CSP power. Solar resources are distributed so widely that multiple potential CSP sites are located near the power grid. Local grid congestion during peak times, however, could play a role, although this factor was not considered here.

A critical aspect of CSP power, however, is the geographical concentration of the suitable resource. The previous calculation was conducted using an aggregate US model. A version of this model with California solar resources specified separately was also created to identify the potential role of solar power in California (Smith *et al.* 2007). While, in that study, the electricity market was still national, the generation of solar (and wind) power as well as the demand for building electricity specifically for the state of California was determined. The result was that the amount of CSP power generated in California

quickly exceeded total California electricity demand. Substantial very long-distance transmission capability would be needed in order to fully utilize the existing solar resource. This implies that the results shown in Figure 5-1 are an overestimate of the CSP penetration as this concentration was not taken into account.

Our conclusion is that CSP solar power systems even without thermal storage have the capability to make a significant long-term contribution to U.S. electricity supply if costs decline to the extent projected. While a carbon tax has some impact on the cost of CSP power due to the operation of the hybrid mode with natural gas (Figure 3-6), the effect is not overly large. A more precise estimate of the role of CSP will require consideration of the geographic concentration of the solar resource (see next section). While the absolute contribution in terms of energy content of CSP technologies, even as shown in the preliminary results in Figure 5-1, is less than that of wind power, CSP is providing firm intermediate and peak power. The value of this technology, therefore, may be higher than its fraction contribution might suggest, particularly since de-carbonizing intermediate and peak power is likely to be more expensive than de-carbonizing baseload power (Wise and Dooley 2007).

5.3 Next Steps

Several analysis steps are necessary to more fully examine the potential role of solar technologies in the U.S. energy system and their role in a carbon constrained world in particular. A key improvement that is already underway is the incorporation of explicit peak, intermediate, and baseload power into the ObjECTS MiniCAM (Wise and Smith 2007) along with the capability of considering electricity storage technologies.

Solar technologies operating during daylight hours will supply primarily intermediate and peak power. The pricing difference between peak and baseload power is likely to be a key influence on the adoption of solar technologies. An explicit market for intermediate and peak power will also more realistically represent the potential contribution of solar technologies without storage.

For CSP technologies, in addition to explicit intermediate and peak markets, the effect of geographic concentration of CSP generation needs to be included in the model. One relatively simple method of doing this would be to estimate the fraction of load that occurs within each CSP resource area and limit CSP penetration to that fraction of the total intermediate and peak demand. Further penetration of CSP would require additional investment (and public and regularly approval) of substantial long-distance electric transmission capability. It may be possible to include this option as well. Whatever

method is implemented for the geographically heterogeneity of CSP will also be applicable for resources used for PV power as well.

More advanced CSP technologies with integrated thermal storage could also be included. CSP with moderate amounts of thermal storage (a few hours) would continue to compete in the intermediate and peak markets. At low penetration levels, it appears likely that, unless integrated thermal storage is sufficiently inexpensive, CSP plants without thermal storage may be economically more competitive. At higher penetration levels it is possible that the advantages afforded by thermal storage in terms of higher energy capture may come into play.

A more substantial amount of thermal storage, for example 8-12 hours, would allow CSP technologies to supply baseload power, thus broadening their potential impact on the electric system. The cost of CSP power, however, would have to be lower to successfully compete with the generally lower cost of other baseload electric generation technologies.

PV technologies can be incorporated into the ObjECTS model as a technology-resource combination with a capacity limit that reflects the need for backup as indicated in Chapter 4 of this document. It would be useful to estimate the correlation of solar irradiance with cooling loads as the electric demand due to cooling load, that is proportional to solar irradiance, would not incur any additional backup requirement.

Modeling of high penetration scenarios for PV will require consideration of storage technologies or the potential "turndown" of baseload technologies. Another possibility that could occur in a carbon-constrained world is the use of intermediate capacity that runs at night but not during the day. This contrasts today's standard practices, but is not unimaginable.

5.4 Summary

The conclusion of our analysis thus far is that CSP solar power systems, even without thermal storage, have the capability to make a significant long-term contribution to U.S. electricity supply. Further analysis will be facilitated by the development, which is underway in 2007, of explicit peak, intermediate, and baseload markets within the ObjECTS MiniCAM, including the capability to model electricity storage technologies. This will enable the realistic analysis of a suite of solar technologies, their potential role in mitigating carbon emissions, and their interactions with a wide range of supply and end-use technologies.

References

Denholm, P. and R. Margolis (2004) "Very Large-Scale Deployment of Grid-Connected Solar Photovoltaics in the United States: Challenges and Opportunities" *Conference Paper, NREL/CP-620-39683*

Kyle, P, SJ Smith, MA Wise, JP Lurz, and D Barrie (2007) *Long-Term Modeling of Wind Energy in the United States* PNNL-16316.

NREL – National Renewable Energy Laboratory (2007). Projected Benefits of Federal Energy Efficiency and Renewable Energy Programs: FY 2008 Budget Request (NREL/TP-640-41347).

Smith SJ, P Kyle, MA Wise, LE Clarke, EM Rauch, SH Kim, JA Dirks, JD Dean, and DB Belzer (2007) *California in a Climate Context: Long Term Scenarios of End-Use Efficiency & Renewable Energy* (PNNL-16607).

Wise, M.A. and J.J. Dooley (2006) "Baseload and Peaking Economics and the Resulting Adoption of a Carbon Dioxide Capture and Storage System for Electric Power Plants" *Greenhouse Gas Control Technologies,* vol **1**, pp. 303-311.

Wise, MA, and SJ Smith (2007) *Integrating Renewable Electricity, Electricity Demand, and Electricity Storage: A New Approach for Modeling the Electricity Sector in ObjECTS* PNNL-16500.